UNIVERSITY OF VAASA
FALCUTY OF TECHNOLOGY
TELECOMMUNICATIONS ENGINEERING

Vo Thanh Vinh

ANTI-SWAY ALGORITHM AND ITS IMPLEMENTATION FOR INDUSTRIAL OVERHEAD AND GANTRY CRANES

Master's Thesis for the degree of Master of Science in Technology submitted for inspection in Vaasa, 1st, May, 2014.

Supervisor Professor Petri Helo.
Professor Mohammed Salem Elmusrati.

ACKNOWLEDGEMENT

I would like to specially express my gratitude to Professor Petri Helo for inaugurating, leading and managing this project. Along the way, he has provided me with all the needed helps, encouragements, technical advises and communications. Therefore, to him I am grateful.

I would like to express my gratitude to Professor Mohammed Salem Elmusrati for giving me wholehearted support and supervision to successfully complete my thesis. Especially, the knowledge that I learnt from him during my education period serves as vital role to the success of the project.

My special appreciation and thanks to Mr. Steve Ekstrom who has also been a leader of this project. His knowledge and passion have been essential for the success of the project.

A special thank goes to Mr. Niklas Envall and Mr. Andreas Ek. Mr. Niklas Envall has been the main engineer in designing and producing process of the anti-sway production board. Mr. Andreas Ek has been responsible for installation and configuration of cranes. In addition, they have always been invaluable source of knowledge for me to consult when I am stuck with problems.

In addition, I would like to credit all members of the Telecommunication and Information Technology Department in the University of Vaasa and Technobothnia Research Centre for maintaining the high quality and comfortable, learning-oriented environment during my period of education.

Vaasa, 1st September 2013

Vo Thanh Vinh

TABLE OF CONTENTS

ABBREVIATIONS AND ACRONYMS

MCU	Microcontroller Unit
CPU	Central Processing Unit
FLC	Fuzzy Logic Controller
RTU	Remote Terminal Unit
CRC	Cyclic Redundancy Check
PLC	Programmable Logic Controller
STRT	Start
STP	Stop
DIR	Direction
EXT	External
REF	Reference
ICSP	In Circuit Serial Programming
ODFC	Output-Delayed Feedback Control
PWM	Pulse-Width Modulation
EEPROM	Electrically Erasable Programmable Read-Only Memory
SRAM	Static Random-Access Memory
TTL	Transistor–Transistor Logic
SPI	Serial Peripheral Interface Bus
I2C	Inter-Integrated Circuit
HTTP	Hypertext Transfer Protocol
FTP	File Transfer Protocol
TCP/IP	Transmission Control Protocol / Internet Protocol
UART	Universal Asynchronous Receiver/Transmitter
ADC	Analog-To-Digital Converter
CW	Clock-wise
USB	Universal Serial Bus

PID	Proportional-Integral-Derivative
FLC	Fuzzy Logic Controller

SYMBOLS

$\theta(t)$	Sway angle from pendulum's equilibrium point at time t.
θ_0	Maximum sway angle from pendulum's equilibrium point.
T	Period of oscillation.
g	Local strength of gravity.
L	Length of the rope that suspends the load of pendulum.
m	Weight of load (of pendulum).
$\vec{a}$	Acceleration vector.
$\vec{v}$	Velocity vector.

UNIVERSITY OF VAASA
Faculty of Technology

Author:	Vo Thanh Vinh
Topic of the Thesis:	Anti-Sway Algorithm And Its Implementation For Industrial Overhead And Gantry Cranes
Name of the Supervisor:	Professor Petri Helo Professor Mohammed Salem Elmusrati
Degree:	Master of Science in Technology.
Department:	Department of Computer Science.
Degree Programme:	Master's Programme in Communications and Systems Engineering.
Major Subject:	Telecommunication Engineering
Year of Entering the University:	2011
Year of Completing the Thesis:	2014 **Pages:** 112

Abstract:

In today's market, due to stiff competition, manufacturers must continuously seek for innovation to increase productivity. One potential area of innovation is improving crane operations. Typically, cranes are used in manufacturing or maintenance processes, where productivity and safety are considered as most important requirements. Load swinging during crane's movement is considered as most severe problem affecting ability to operate crane efficiently .Production queue delay can be greatly reduced if crane sway control is implemented properly.

In this paper, the crane load sway phenomenon is modeled and analyzed in depth. As the result, a new solution to suppress load sway is proposed. In contrast with various existing anti-sway solutions, our solution is easy to deploy, fast to converge and independent with load weight as well as crane's rope length. Moreover, the solution is also very affordable and suitable for most of existing motor drive models .The solution is theoretically verified by simulation with software physics engine. Lastly, several anti-sway hardware prototypes were developed and tested against a real overhead crane in factory. The proposed anti-sway algorithm has been proven to be very effective in minimizing load sway to increase speed and reliability in crane operation.

Keywords:

Overhead Crane, Load Sway, Anti-sway, Kalman Filter, Modbus, Inclination Sensor, dsPIC33F, ABB ACS800, Arduino, ASM PTAM27, ADIS16029, ST485, Box2D.

1. INTRODUCTION

1.1. Background

Nowadays, cranes are very popular equipment in factories. They are part of everyday work to move heavy objects between production lines. Cranes can be found in metal factories, car industries, loading and unloading ships, machinery factories….In many cases, the efficiency of production is decided by how fast load-moving operation is. Therefore, many factory-owners have been investing money and effort in order to improve the safety, consistency and velocity of their cranes.

There are many problems associated with improving the operation of cranes .However, the sway of load carried by crane during movement has always been the most classical and challenging problem in crane movement. Heavy-load sway can cause serious damage in property and human injury if accident happens. Without the help of anti-sway solutions, crane operators need to control crane based solely in feeling, observation and experience. Workers need to have certain level of expertise and experience to be qualified to control cranes. Anti-sway solutions can vastly reduce the risk of accidents and improve speed as well as reliability of crane operation. Workers with basic training can operate crane safely with the help of anti-sway algorithm.

In this thesis, I will focus on developing and analyzing an innovative solution to counter sway when operating an industrial overhead or gantry crane. The solution is promised to be effective and inexpensive in term of implementation, integration and maintenance. Moreover, since we are developing systems for industrial environment, there is certain level of robustness we need to fulfill such as: dust, water, electrical noise, wide range of temperature… These standard requirements are also taken into account when designing the solution.

In addition, because of the option of replacing the old motor drive with newer one is often too expensive and complicated to be considered by factory-owner, the proposing anti-sway

solution will be convenient and simple to be able to integrate with not only modern cranes but also legacy crane systems. In fact, the solution is designed as a plug-in system for existing cranes. By using plug-in design, the solution can support various crane vendors and can be highly customizable and extendable. At the end of the thesis, some extended possibilities of the solution will be introduced to readers.

1.2. Objective of the project

The thesis will mainly focus on developing an inexpensive, effective and convenient solution for minimize the effect of load sway in industrial crane operation. This project, apart from promoting academic knowledge gained from my education, has practical impact to production's efficiency and safety if it is applied successfully. Manual controlling of the crane can be replaced with computer-aided system to improve speed and reliability. Target of the project is to fulfill following requirements:

- Develop effective algorithm to reduce load sway of cranes.
- Simulate the system using physics engines.
- Build a working prototype including hardware and software to demonstrate the concept.
- Testing of prototype with actual crane.

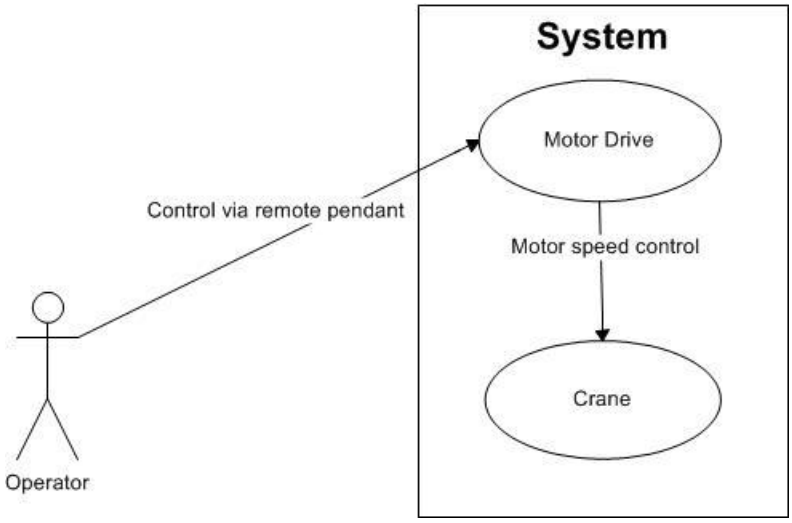

Figure 1. Use case without anti-sway device.

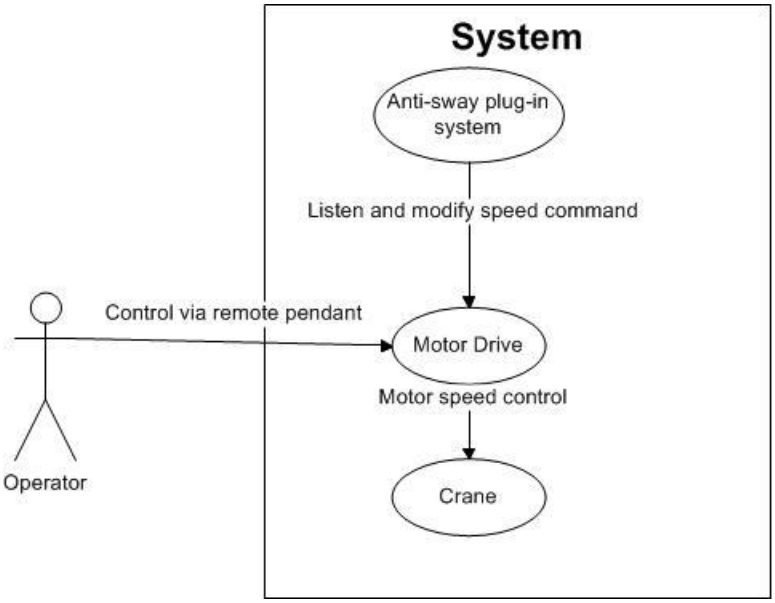

Figure 2. Use case with anti-sway device.

The anti-sway module will act as a plug-in to existing crane system as demonstrated by the user cases in Figure 2. The module will be integrated with motor drive and remote controller to listen and modify speed command for the motor via motor drive to reduce the sway effect during operation.

The thesis will be presented in following structure:

- Overview of related works.
- Modeling of industrial crane and its load-sway problem.
- Detailed requirements of the anti-sway module.
- Detailed anti-sway algorithm is proposed and analyzed.
- Simulation of algorithm is implemented by computer using physic engines to demonstrate its effectiveness.
- Conceptual hardware design.
- Test case implementation of software and hardware for crane with ABB ACS800 drive.
- Test results are presented.
- Future work and possibilities.

1.3. Overview of related works

There has been significant research effort on minimizing sway effect of cranes. As a result, there is wide range of solutions using various mechanical structures, sensor inputs and controlling methods to address the problem. Popular existing anti-sway solutions will be examined in this session.

1.3.1. Mechanical-based solutions

In this type of solution, additional mechanical structure was installed to the crane to maximize the damping effect of crane's oscillation.

One example solution is to install a small auxiliary mass to the spreader of the crane in combination with closed loop system such as H_∞ controller (GB. Kang et al.., 2003) or gain scheduling controller (Dong Kyu Kim et al., 2005).

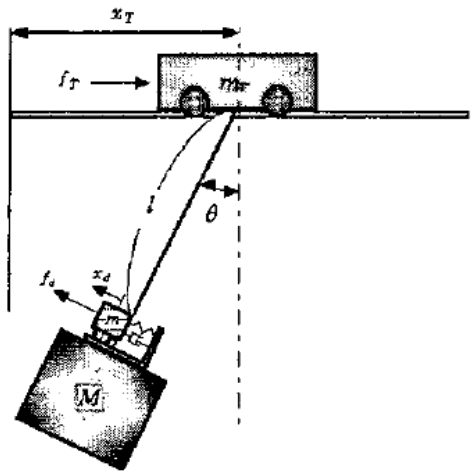

Figure 3. Crane with additional auxiliary mass (GB. Kang et al.., 2003:2)**.**

In above solution, a rather complex auxiliary structure was required to be installed to the spreader. The installation of the auxiliary mass is not always possible for all types of hook/spreader. Moreover, spring damping effect is very slowly convergent. As the result, sway effect is killed off slowly. In Figure 4 and Figure 5, it takes approximately 10 seconds to stabilize the load. Moreover, he crane can't be stopped effectively without a long delay because of slow convergence. Lastly, system parameters depend on load mass and rope length measurements which are usually vary from operation to operation.

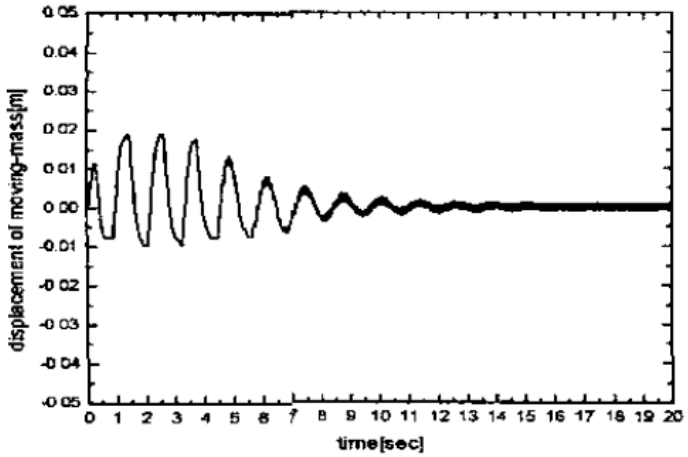

Figure 4. Displacement of moving mass (GB. Kang et al.., 2003:4)**.**

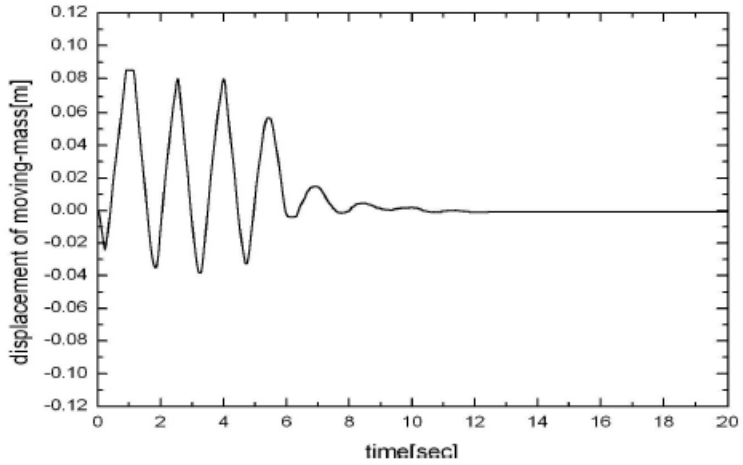

Figure 5. Displacement of moving mass (Dong Kyu Kim et al., 2005:5)

1.3.2. Sensorless solutions

The main advantage of sensorless solutions is easy configuration which requires no additional hardware or structure to be installed. However, this type of solution has many disadvantages:

- Slow convergence of oscillation. This problem will cause crane movement to be instable and stopping process will be slow as well.
- Adaptability of the system to inconstant system parameters such as rope length and load weight. The controller requires an estimation of system parameters to effectively model the system. Parameters such as rope length and load weight can change greatly and they are not very easy to measure in real system.

Input Shaping Controllers (Neil Singer et al., 1997) is an example solution that requires no sensor to minimize swinging effect. This is among most popular methods to control cranes. However, the system greatly depends on rope length parameter and it is also slowly convergent.

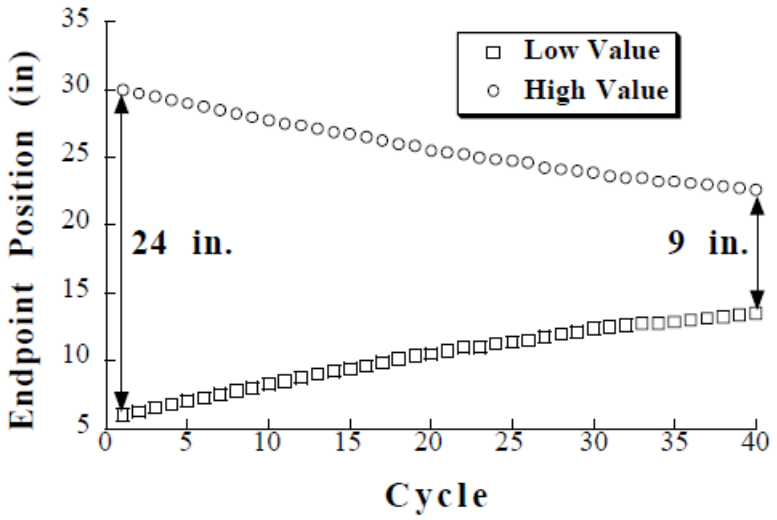

Figure 6. Measured Peak-to-Peak Oscillation (Neil Singer et al., 1997:5).

1.3.3. Sensor based solutions

Sensor-based solution consists of a sensor system and a closed-loop controller to stabilize crane. Popular sensor systems include: vision system - camera with image processing software (K. S. Hong et al., 2004; Hideki Kawai et al., 2009), acceleration sensor (Ki-Ru Park et al., 2010) or inclination sensor (Y. S. Kim et al., 2004). Among these, vision system is very expensive and difficult to maintain. Moreover, vision system doesn't work well under certain conditions such as rainy days or dusty environment. Therefore, vision system is considered to be the least effective sensor system. Popular controllers which are used along with sensor feedback are listed as follow:

- Nonlinear controllers: Nonlinear coupling controller (Y. Fang et al., 2003), Second-order sliding-mode controller (G. Bartonlini et al., 2002), Output-Delayed Feedback Control (Rajeeb Dey et al., 2010), Fuzzy Controller (Shu-jiang Li et al., 2005).

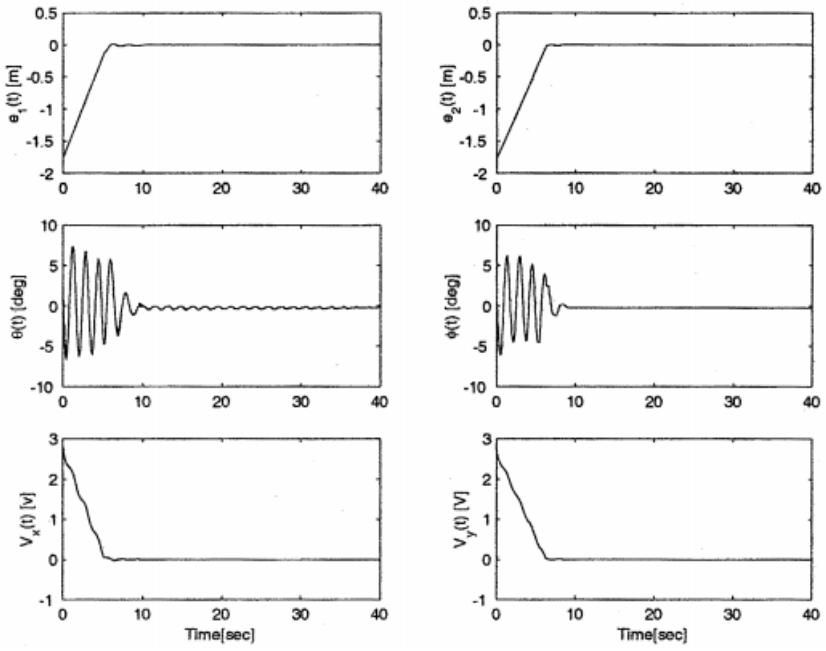

Figure 7. Results for the gantry kinetic energy coupling control law (Y. Fang et al.,2003).

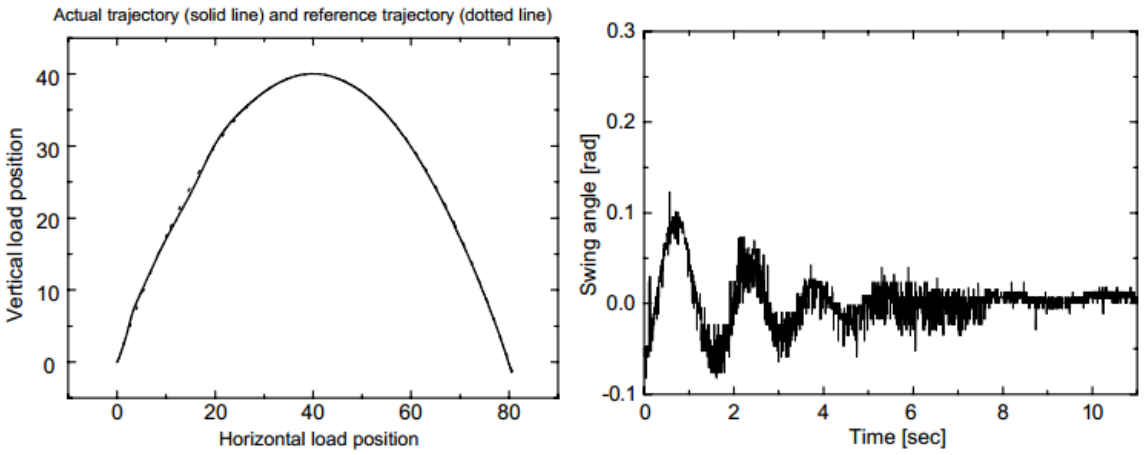

Figure 8. Result for second-order sliding-mode control (G. Bartonlini et al., 2002).

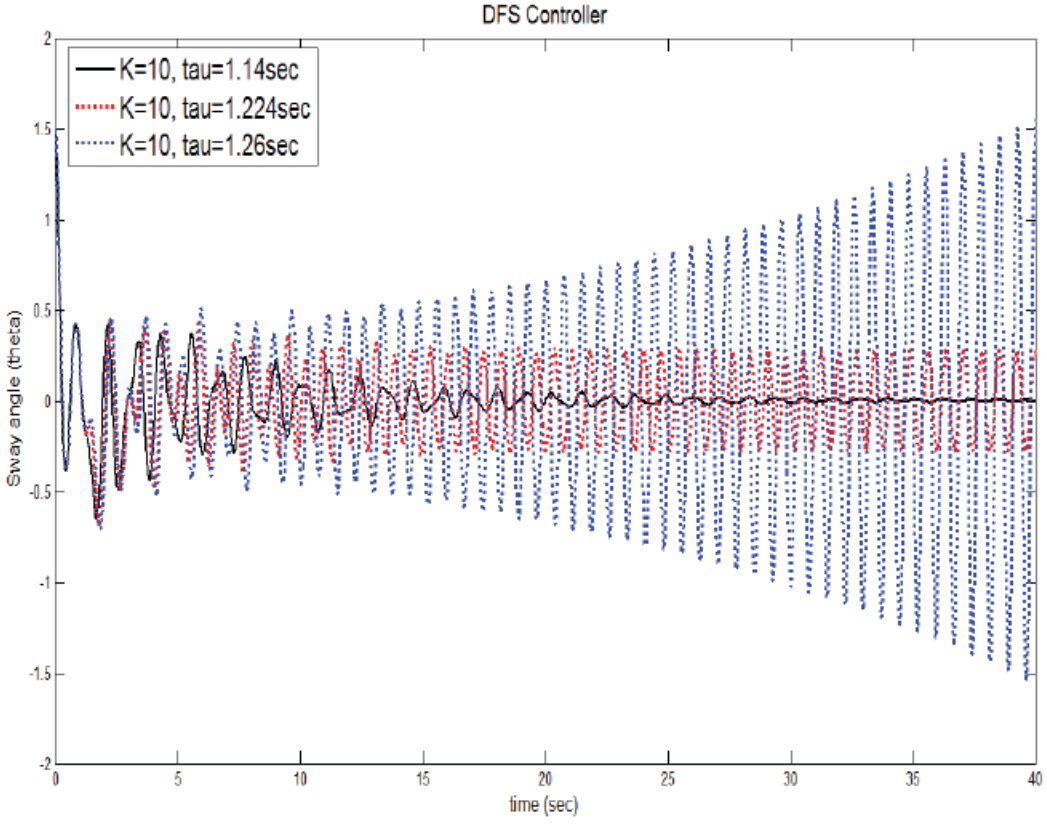

Figure 9. Result for Output-Delayed Feedback (Rajeeb Dey, 2010:4).

Non-linear controller convergence speed has been improved in comparison with other types of controllers. However, it still takes some oscillation circles to reach its convergent state.

- Linear controllers. PID-based is the most popular in this controller category, PID controller is very robust against external disturbance factors and changes of system parameters. However, it still has the disadvantage of slow convergence.

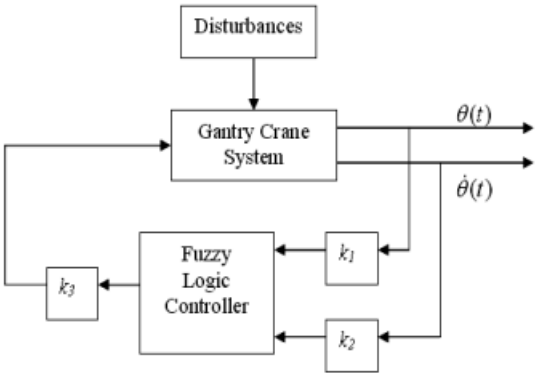

Figure 10. PD type Fuzzy Logic Controller (M.A. Ahmad, 2009).

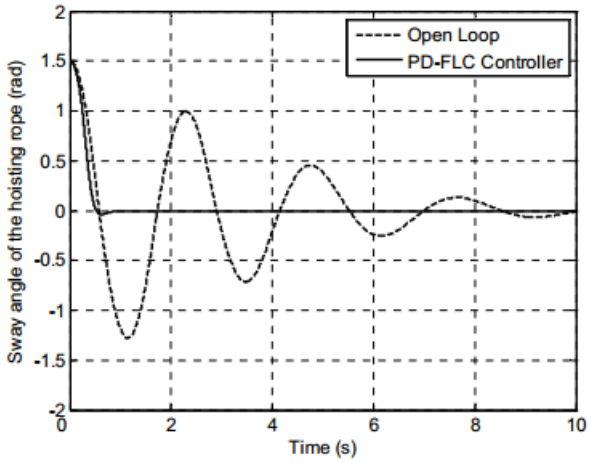

Figure 11. Sway angle of the hoisting rope response with PD-type FLC (M.A. Ahmad, 2009).

1.3.4. Conclusion of previous works

In this section, popular controlling methods of crane has been briefly described and analyzed. Major problem of these controlling methods is that they take a long period of time to achieve the convergence - stable system without sway. Some solutions have been proven to be expensive, difficult to maintain and not reliable under some conditions (bad weather, dusty environment …). In addition to those disadvantages, most of previous solutions depend heavily on system parameters which are not always constant and easy to measure. Therefore, the target of this thesis project is to address those disadvantages and propose an inexpensive, maintainable, stable and most importantly, fast convergence.

2. MODELING OF INDUSTRIAL CRANE AND ITS LOAD-SWAY PROBLEM

2.1. Introduction to gantry and overhead crane

Overhead crane is the type of cranes consists of: parallel runways, crane bridge connecting runways, hoist for lifting. As a result, overhead cranes can move load in 3 dimensions: up and down, along the runways and along the bridge. This type of crane is very popular inside factories due to its multi-directional movement ability.

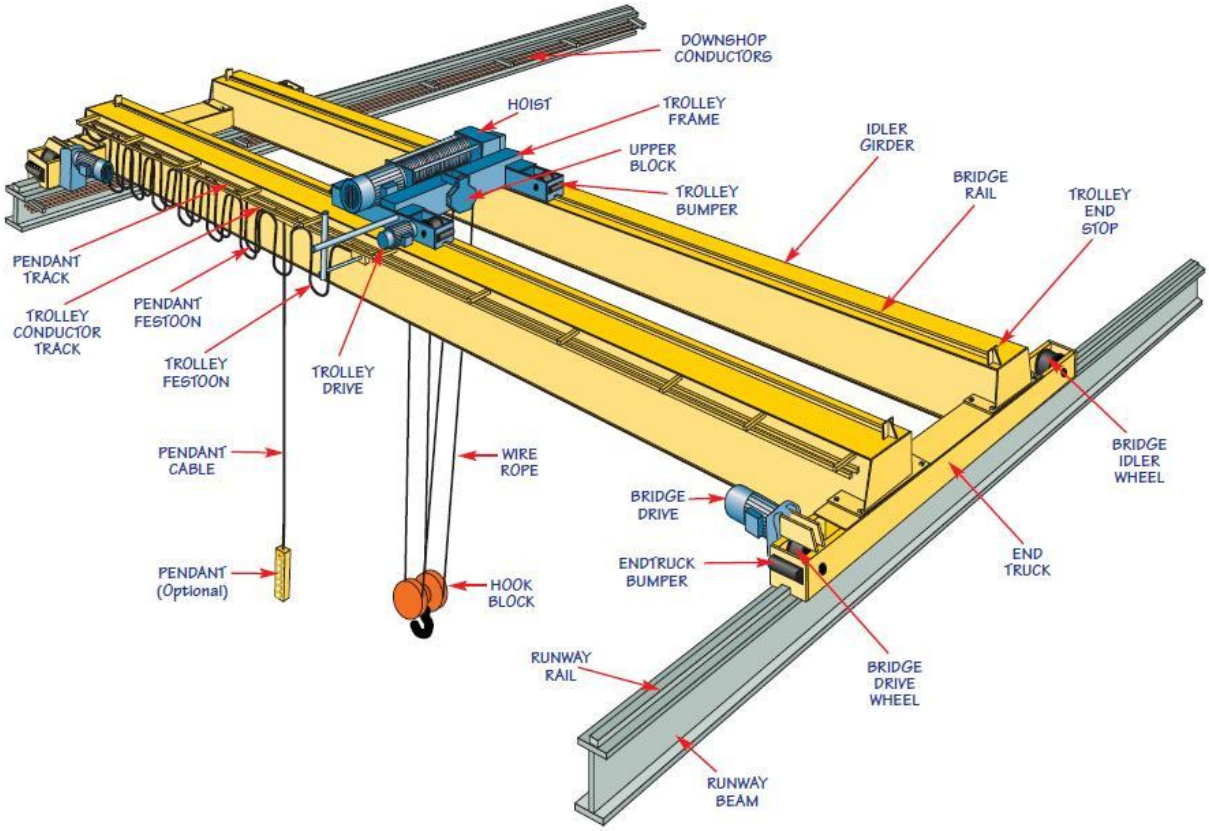

Figure 12. Crane structure (Baoding Weyou Technology Company, *EOT Crane*).

Gantry crane is very similar to overhead crane. However, it does not have the parallel runways which restrict the movement in 2 directions: up and down, along the bridge. Gantry cranes are very popular outside manufacturing factories.

The movement of cranes is enabled by motors. Motors are controlled by motor drive, also known as motor controller or frequency converter. Motor drive can control speed, acceleration, torque and various other attributes of a motor.

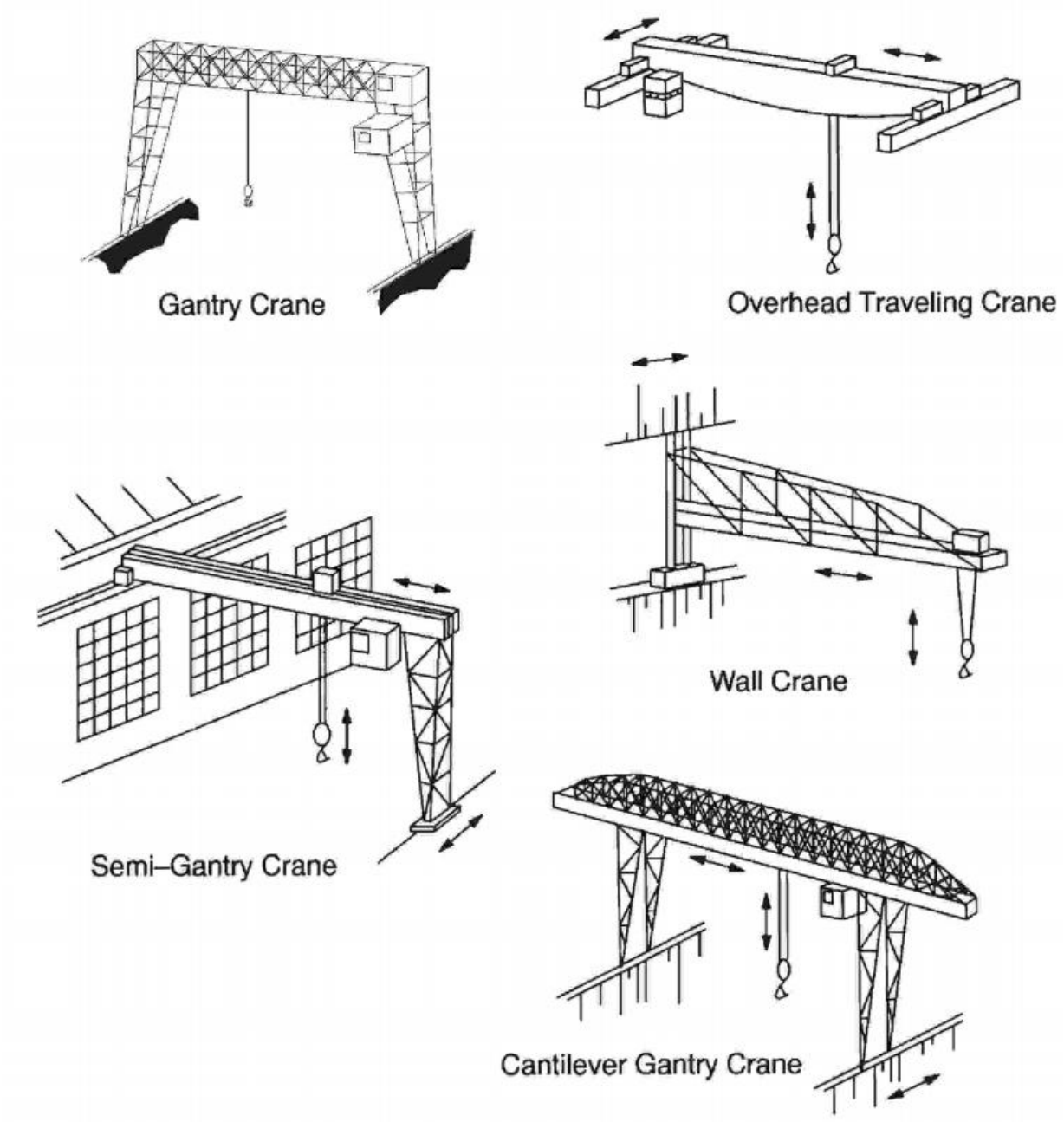

Figure 13. Different types of overhead and gantry crane (U.S. Department of Energy, 2007. *DOE Standard Hoisting and Rigging*).

2.2. Physics model of crane

Moving crane with heavy load can be modeled as a pendulum with movable pivot point.

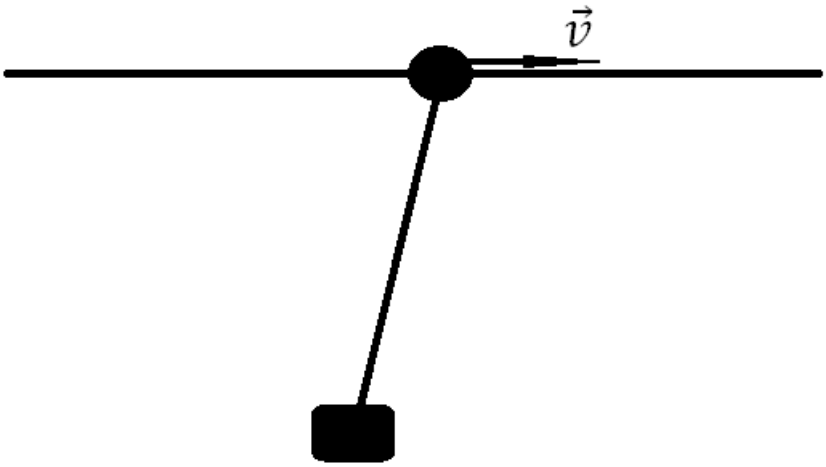

Figure 14. Moving crane physics model.

For small swing amplitude, we have following formulas for pendulum:

- Harmonic oscillation formula:

$$\theta(t) = \theta_0 \sin\left(\frac{2\pi}{T}t\right) \tag{2.1}$$

$\theta(t)$ is the sway angle from pendulum's equilibrium point at time t.

- Approximated formula of oscillation period can be expressed as:

$$T \approx 2\pi\sqrt{\frac{L}{g}} \ \ with\ the\ condition\ of\ \theta_0 < 1\ rad \tag{2.2}$$

T is the period of oscillation.

L is the length of the rope that suspends the load.

g is the local strength of gravity.

θ_0 is the maximum sway angle from pendulum's equilibrium point.

Although above formula is standard for theoretical pendulum, it is not realistic to assume the condition of maximum swinging angle is met during crane's movement. Therefore, approximated formula of oscillation period is not applicable for crane.

However, the crane still possesses symmetric oscillation properties of the standard pendulum which we will exploit to solve the swinging problem of the crane.

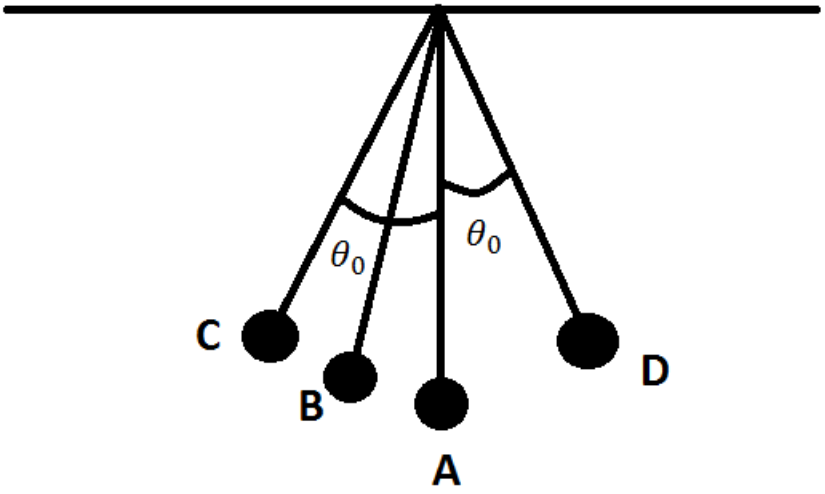

Figure 15. Symmetric oscillation of pendulum.

The symmetric oscillation property can be demonstrated with following examples (with reference to above figure):

- Time to oscillate from A to B will be same as from B to A.
- Time to oscillate from A to C will be same as from A to D, or from D to A, or from C to A.
- Time to oscillate from C to B will be same as from B to C.

Those are some typical examples to demonstrate symmetric oscillation property of crane models.

2.3. Observational frame of reference in crane physics model analysis

Throughout the analysis of crane's physics model, we will use crane's hoist as observational frame of reference. It means that we will observe the swinging phenomenon of the crane as if we are attached to the crane's hoist. Moreover, positive direction of coordinate system will be from left to right.

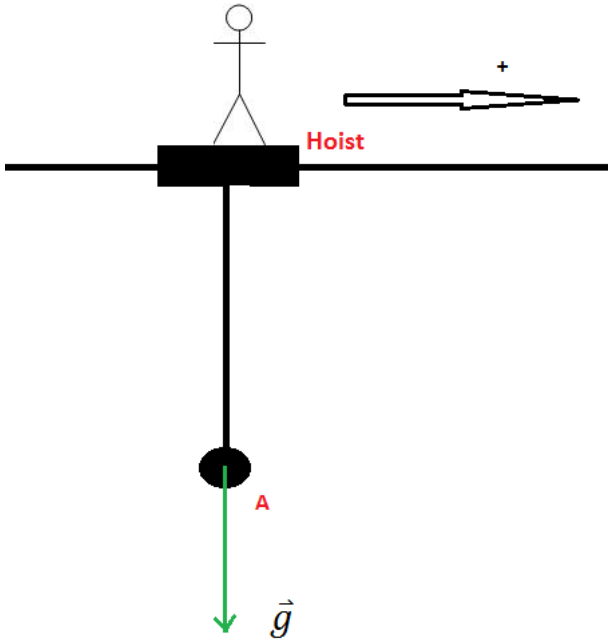

Figure 16. Observational frame of reference attached to the hoist and positive direction is from left to right.

The swinging phenomenon is actually the movement of the load in reference to the hoist. Therefore, the choice of using the hoist as reference coordinate system is logical.

It is worth noticing that: if the hoist is accelerating with acceleration $\vec{a}$ and we are using the hoist as observational frame, the load will look as if it suffers from a force $-m\vec{a}$ from our observational frame of reference (David Morin, 2008: 457 – 500).

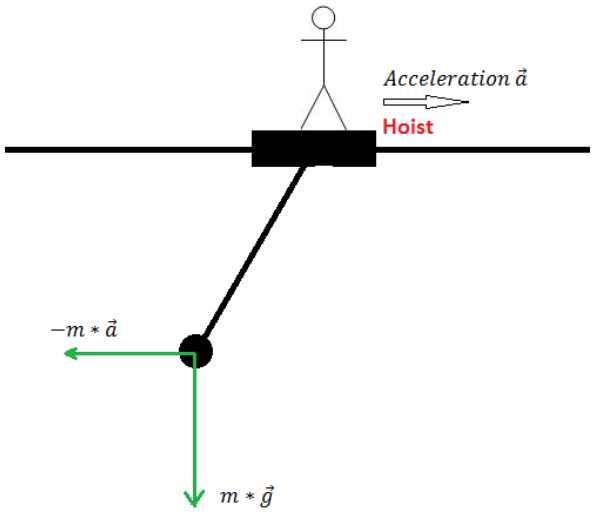

Figure 17. Observational frame of reference attached to the hoist.

The convention in which observational frame of reference is attached to crane's hoist will be used throughout this paper.

2.4. Sway analysis of moving cranes

The crane movement is divided into three separated periods:

- Ramping up period: during this period the motor will accelerate according to acceleration parameter configured in motor drive.
- Constant speed period: after ramping up period, the motor will reach maximum speed configured in motor drive. The motor will be kept at constant maximum speed until user decides to stop the movement.
- Ramping down period: this is stopping period of the crane. The crane speed will be decelerated according to deceleration parameter configured in motor drive.

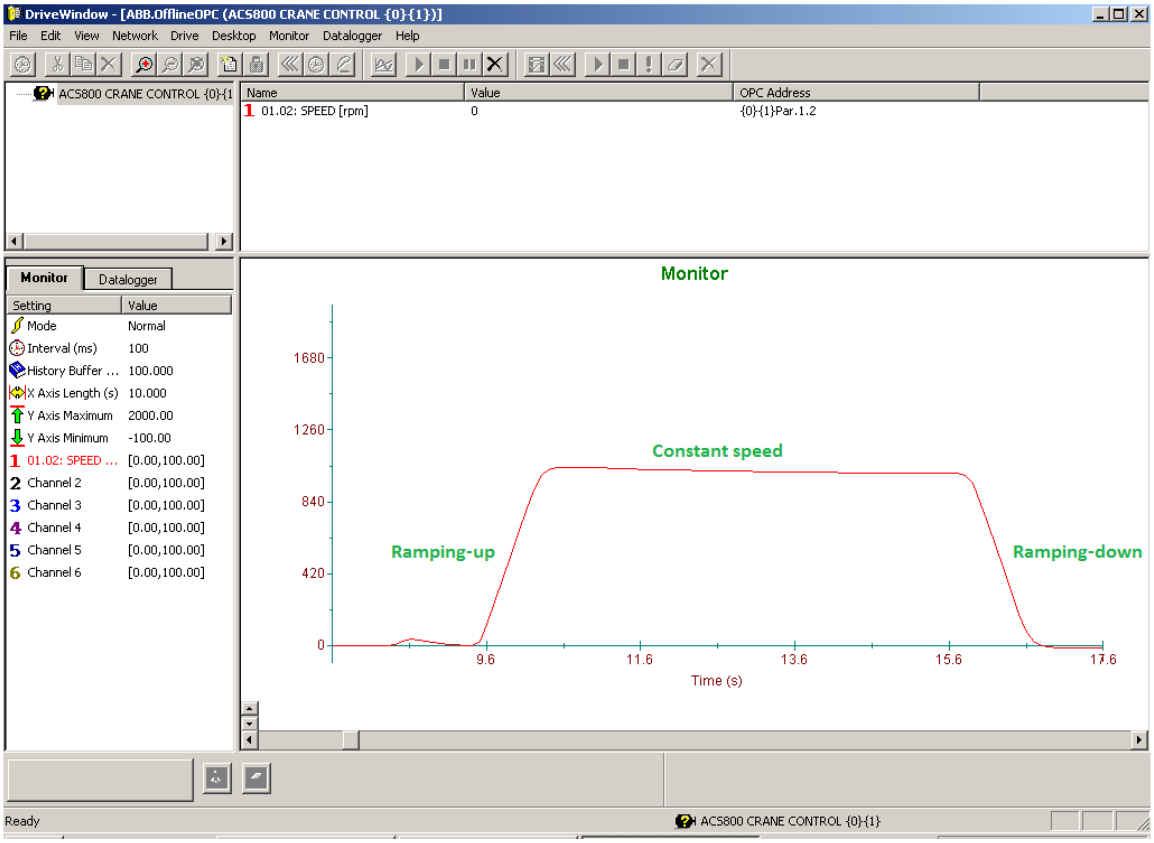

Figure 18. Speed diagram during crane's movement (taken from ABB ACS800 motor drive).

At beginning, let's assume that the load is at its normal equilibrium position as follow:

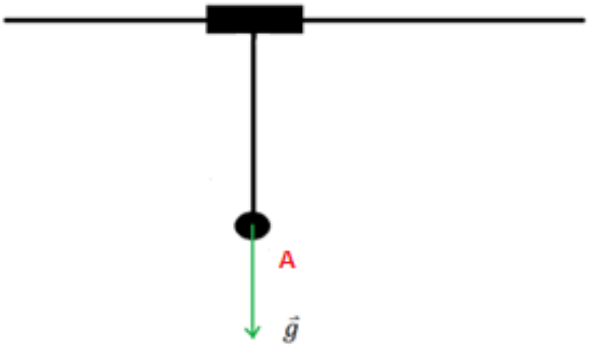

Figure 19. Crane at equilibrium position.

The load sway is initiated during the ramping up period.

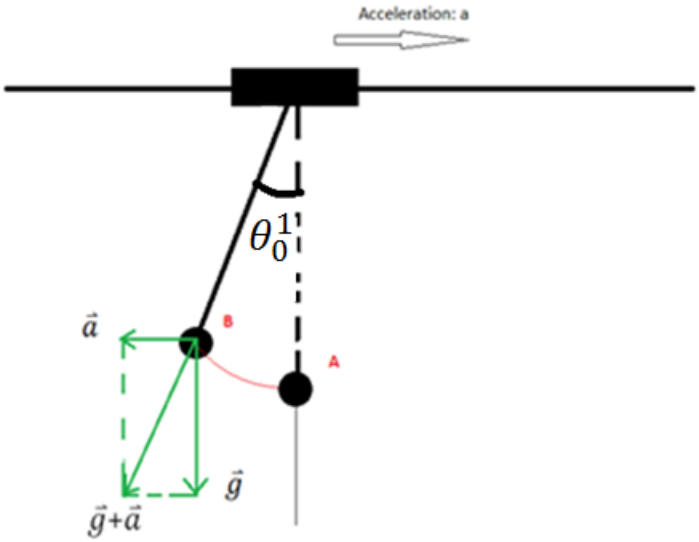

Figure 20. Crane during acceleration.

During ramping up period (with acceleration $\vec{a} > 0$), the equilibrium position is changed from A to B as above. As the result, crane's load will start to oscillate around new equilibrium point B (with maximum angle θ_0^1) during ramping up period.

Suppose that at the end of the ramping-up period (at the beginning of constant speed period), the load is at C position like in the figure below:

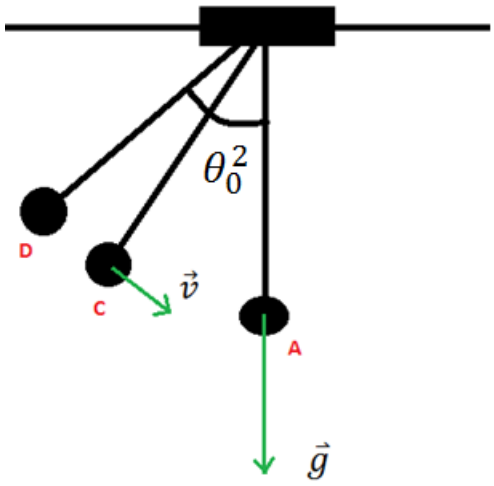

Figure 21. Load sway after acceleration.

Within the constant speed period ($\vec{a} = 0$), the equilibrium position is changed back to A. At C, the load has velocity resulted from ramping-up period's oscillation. Therefore the load will oscillate at even greater amplitude around A. As a result, the load will oscillate around A with maximum angle θ_0^2 for the rest of constant speed period.

Suppose that at the end of the constant speed period the load is at F position like the figure below:

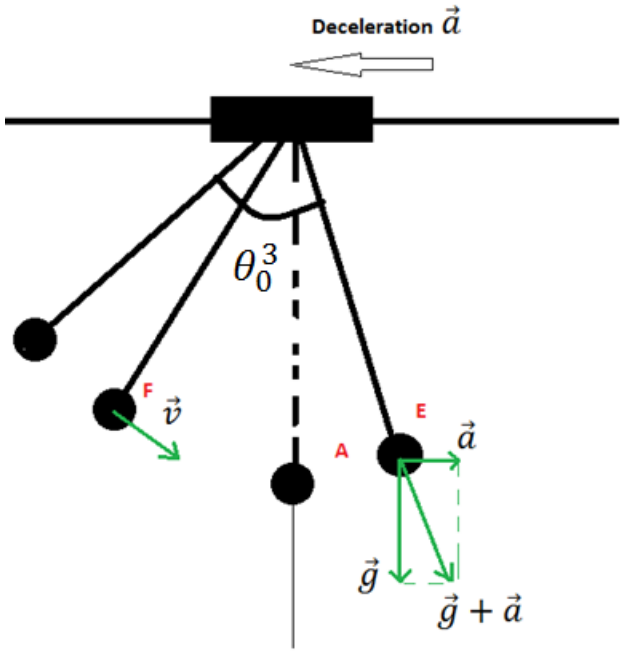

Figure 22. Load sway during deceleration.

In the ramping down period (with acceleration $\vec{a} < 0$), the equilibrium point is now E in figure above. The load, at the end of constant speed period is at F with certain velocity. As a result, during ramping down period, the load is oscillating around E with amplified maximum angle θ_0^3.

Suppose that at the end of the ramping down period, the load is at G position with certain velocity like in the figure below:

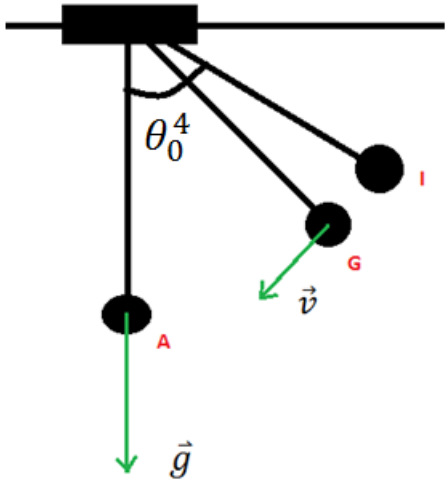

Figure 23. Load sway after deceleration.

When the crane is stopped, the pendulum‘s equilibrium position is once again changed back to A. At the end, the load will oscillate around A position with maximum angle θ_0^4.

In brief, during all periods of crane’s movement, swing happens as the result of changing equilibrium position. Moreover, swing amplitude is magnified when crane is switching from one state to another (ramp-up → constant speed → ramp-down).

2.5. Conclusion

In this chapter, overhead crane as well as gantry crane were introduced and compared with each other. Both mentioned types of crane are affected by load swinging problem during operation. In order to analyze swinging problem, physics model of crane is presented based on a standard pendulum. However, small swing pendulum’s calculations are not applicable to our crane model because it is not feasible to assume small swing during crane’s movement. At the end, the analysis of crane motion demonstrates how swing happens and how swing amplitude is amplified during movement’s process.

3. ANTI-SWAY ALGORITHM

3.1. Introduction and requirements of the anti-sway algorithm

The algorithm was developed in order to minimize swing of load for crane movement under the control of operator.

Algorithm‘s requirements are listed as follow:

- The speed control commands must be simple so that motor drive can perform effectively.
- The algorithm needs to take into account that crane might be carrying heavy load that it is not possible to change speed very frequently.
- Approximated formula such as $T \approx 2\pi\sqrt{\frac{L}{g}}$ is not applicable because small swing is not guaranteed.
- Rope’s length and load’s weight are not available for algorithm because we want algorithm to be able to perform well with variable load’s weight and rope’s length.
- All motor drive’s parameters are available to algorithm to utilize such as: current measurement of speed, speed settings (such as: step speed, max speed, min speed, etc), digital IOs, …
- Algorithm can send start/stop/set speed command to motor drive.
- The inclination (or angle) of the crane’s rope will be made available for no-swing algorithm by a sensor.
- The algorithm will be implemented using microcontroller.

3.2. Crane’s oscillation propositions

3.2.1. Oscillation when trolley has no acceleration

At normal condition (the trolley has no speed or constant speed), a pendulum will oscillate around the equilibrium position as following figure due to gravity:

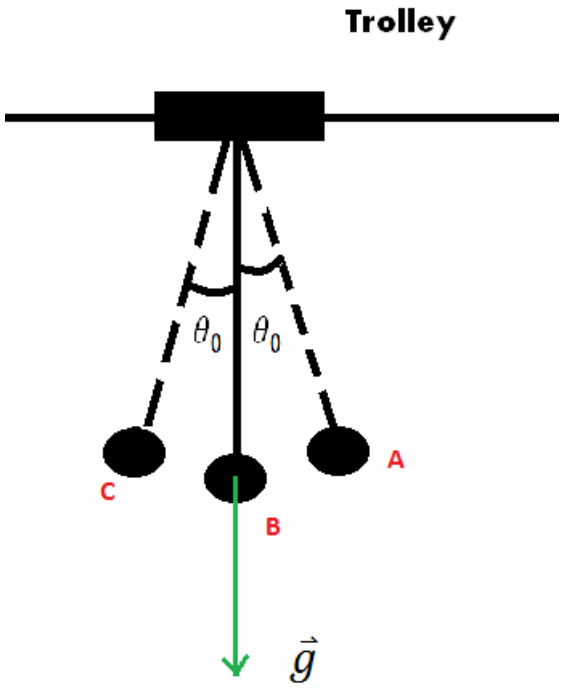

Figure 24. Crane oscillation during stable situation.

This condition is named as stable situation.

3.2.2. Oscillation during trolley acceleration/deceleration

In the situation which the trolley is accelerating with acceleration of $\vec{a}$, if we are taking the trolley as observational frame of reference (which basically means we are standing on the trolley), we will see the load swinging around another equilibrium position(named B in the figure) as follow:

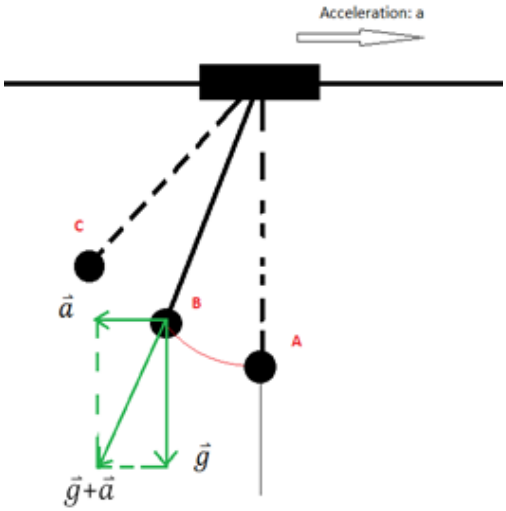

Figure 25. Crane oscillation during acceleration situation.

Moreover, if at beginning of the acceleration process, the load has no oscillation and velocity, the lowest point (named A in above figure) and highest point (named C in above figure) are θ_0 positions (maximum angle positions). As a result, velocity at A, $v_A = 0$ and velocity at C, $v_C = 0$ during oscillation period around B.

Let's name this accelerating situation. If we apply this with a=0, we will have situation described in "3.2.1. Oscillation when trolley has no acceleration", in which the trolley is moving at constant speed.

Same argument is applied for deceleration situation:

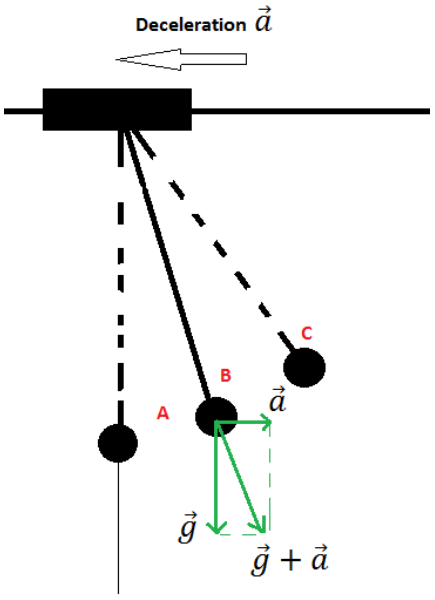

Figure 26. Crane oscillation during deceleration situation.

3.2.3. Symmetric property of oscillation

Oscillation is a function of *sine* or *cosine*. As a result, oscillation is a symmetric movement between two random positions. (Randall D. Knight, 2012: 378–406).

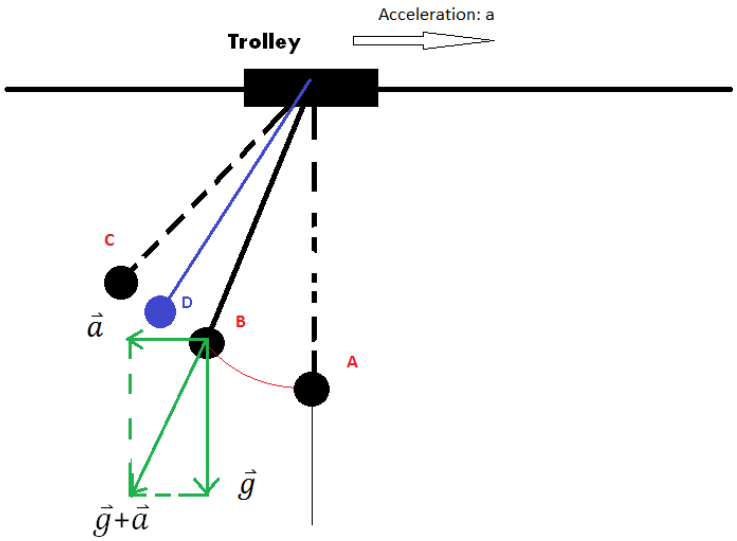

Figure 27. Symmetric oscillation around point B.

Therefore we will have following facts:

- Time taken to travel from A→B→D will be same as D→B→A
- Time taken to travel from A→B→D→C→D will be same as D→C→D→B→A.
- Velocity at certain position does not depend on moving direction. For example: velocity at point B when load is moving to the left is the same at velocity at point B when load is moving to the right.

In other words, time taken for travelling from one point to another is independent of moving direction during symmetric oscillation.

3.3. Anti-sway algorithm mechanism

3.3.1. Ramping up period

Based on theoretical analysis, following speed control pattern is proposed in order to reduce swing when ramping up.

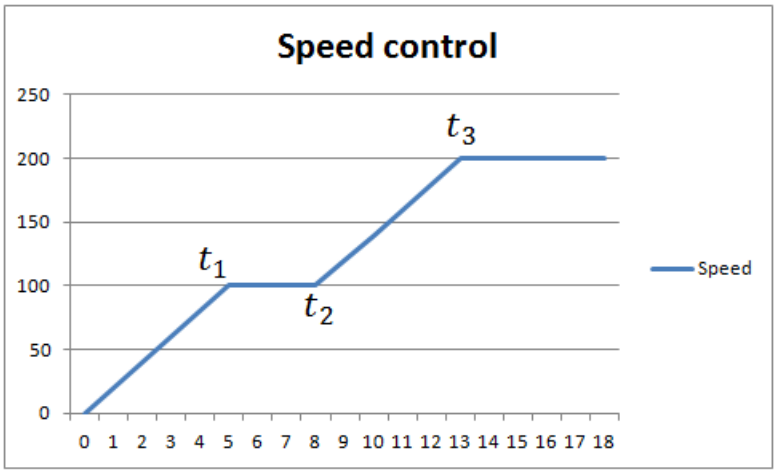

Figure 28. Speed control during ramping-up.

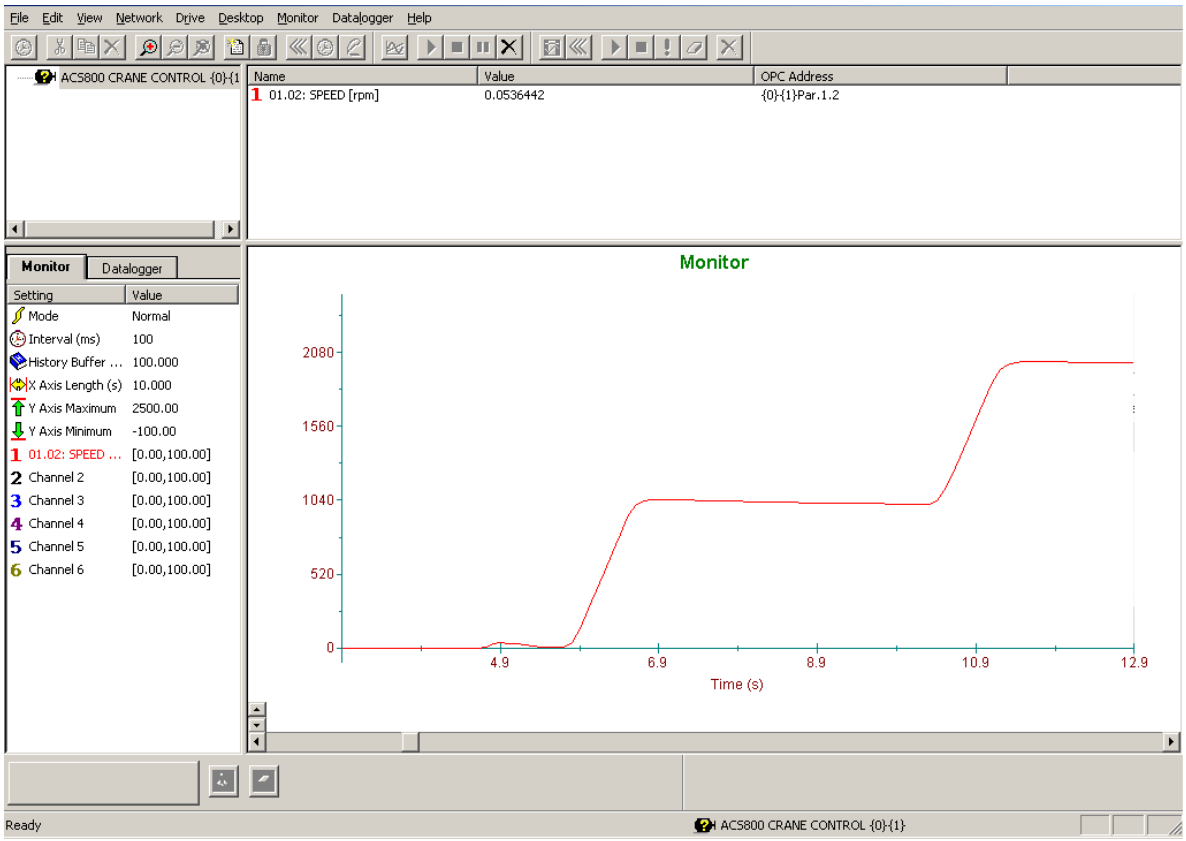

Figure 29. ABB ACS800 ramping-up.

The above figure shows the process when the motor is accelerating (ramping up). Motor deceleration (ramping down) will be controlled in same manner.

In this control pattern, we have three time marks: t_1, t_2 *and* t_3.

- From 0 to t_1 : motor will accelerate/ramp-up from 0 to half of target speed. The speed that the crane will achieve during constant speed period is called *target speed*.
- From t_1 to t_2: motor will keep constant speed.
- From t_2 to t_3: motor will accelerate/ramp-up to target speed.

The first period from 0 to t_1 is trivial. The algorithm will send a start command and set speed to half of target speed in motor drive. Then motor drive will ramp up its motor according to pre-defined acceleration parameter.

The third period from t_2 to t_3 is very similar to first period mentioned above. The algorithm will set speed to full target speed in motor drive. Then motor drive will ramp up its motor according to pre-defined acceleration parameter.

The critical period is from t_1 to t_2, the second period of the whole ramping-up process. In fact, the algorithm is all about deciding how long this period should be to effectively prevent oscillation/swing.

From 0 to t_1, the load will oscillate around point B with A and C as θ_0 positions (maximum angle positions). (Refer to "3.2.2. Oscillation during trolley acceleration/deceleration").

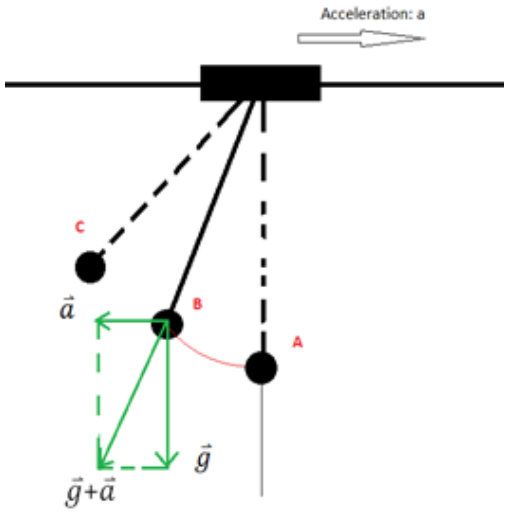

Figure 30. Oscillation around equilibrium point B during acceleration.

Let's suppose at t_1, our load is at point D in the following figure:

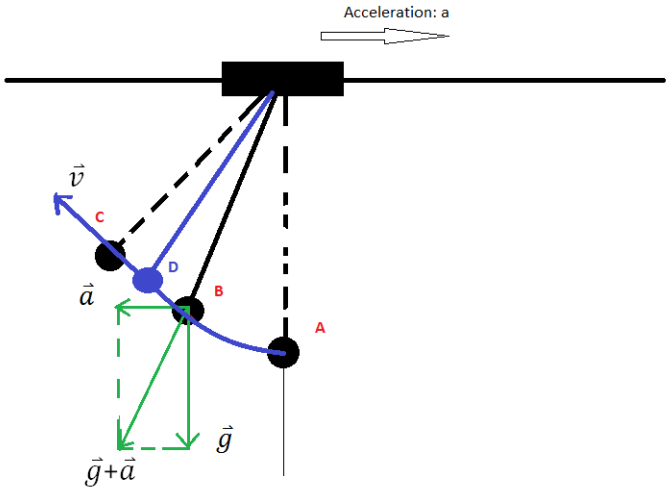

Figure 31. Load is at random position point D during acceleration.

After t_1, the motor will be kept running at constant speed. The load with its current speed will now oscillate around point A (refer to "3.2.1. Oscillation when trolley has no acceleration"). The load will go up a bit more and return to D with exactly same speed in reversed direction (refer to "3.2.3. Symmetric property of oscillation"). At the moment when the load is moving back to D again in reversed direction like following figure:

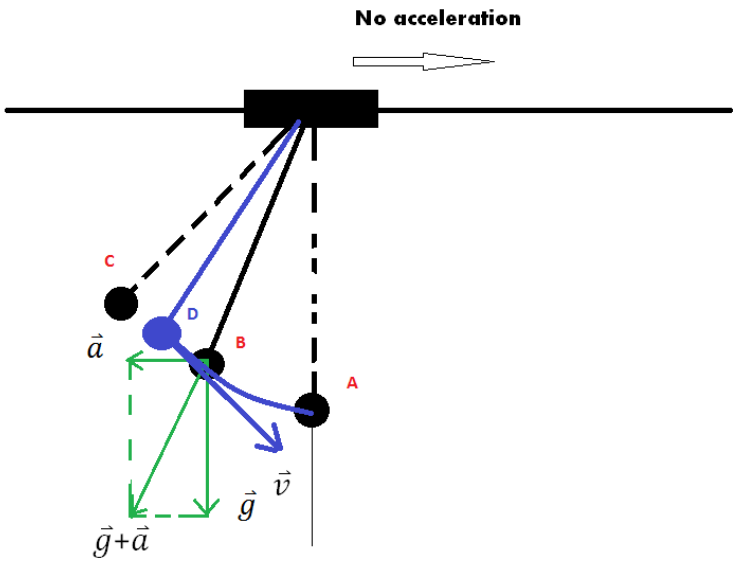

Figure 32. Load is at position point D again (in reverse direction).

Right at this moment (t_2), the motor drive‘s speed parameter will be set to full target speed. The motor will be ramped up to target speed.

When the crane reaches target speed (t_3), the load will be exactly at point A with zero velocity.

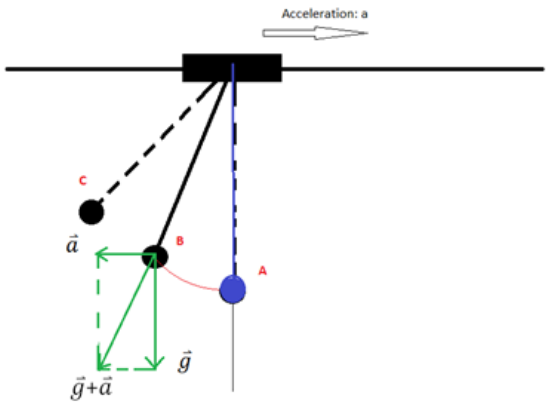

Figure 33. Load at position point A with zero velocity.

How do we know at t_3, the load will be at A? Because average acceleration $\vec{a}$ is constant, we have: $t_1 - 0 = t_2 - t_3$. (Time to accelerate from 0 to half of target speed is same as time to accelerate from half of target speed to full target speed).

$$\Delta t = \frac{\Delta v}{a} \tag{3.1}$$

Δt is duration of period.

Δv is change of speed.

a is acceleration.

While oscillating around B, it takes t_1 to travel from A→D, so D→A will take same time $(t_3 - t_2)$. Moreover, from t_2 to t_3, the load is oscillating around B with A as θ_0(maximum angle). Therefore, at A, velocity will equal zero (At maximum angle, oscillation has no speed).

At t_3 when the load is at A with zero speed, the crane will move with constant target speed. It means that the load oscillate around A (refer to "3.2.1. Oscillation when trolley has no acceleration") with both initial position and speed are zero. As the result, after t_3, all oscillation is killed.

Notes:

At t_1, the position of the load can be like following figure where the load has already reached C and it is going back towards A.

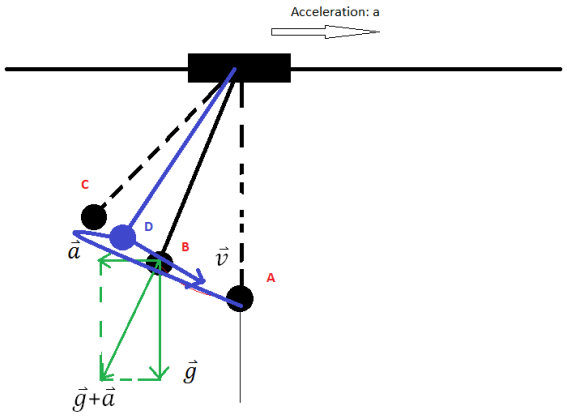

Figure 34. Load at position point D and going towards A (positive speed).

Then we need to keep the motor running at half of target speed until the load reaches D position in reversed direction again like following figure:

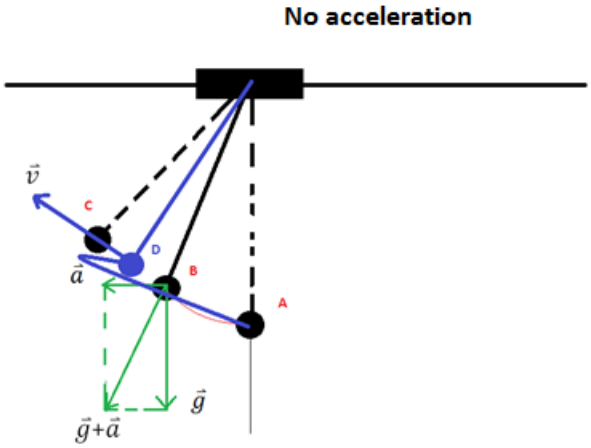

Figure 35. Load at position D and going towards C (negative speed).

When oscillating around B, time needs to travel A→B→C→D (t_1) will be same as D→C→B→A ($t_3 - t_2$).Therefore, at t_3 , the load will end up being at A with zero speed. Finally, after t_3 , all the oscillation will be killed.

In short, if at t_1 the load is at a particular point D, the motor will be kept running under constant speed (half of target speed) until the load is at D again in reversed direction (t_2). After that the crane will be accelerated up to target speed (t_3). Then, constant target speed is used for the rest of the movement. At the result of holding period (from t_1 to t_2), the oscillation will be fully eliminated during constant speed period.

3.3.2. Ramping down

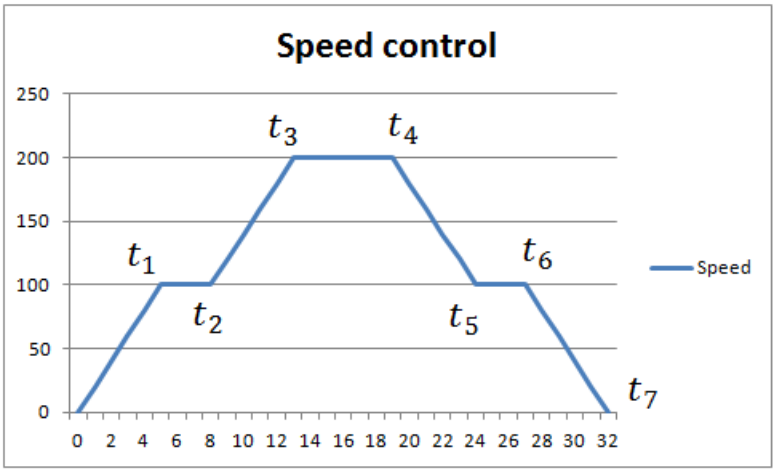

Figure 36. Anti-sway speed control.

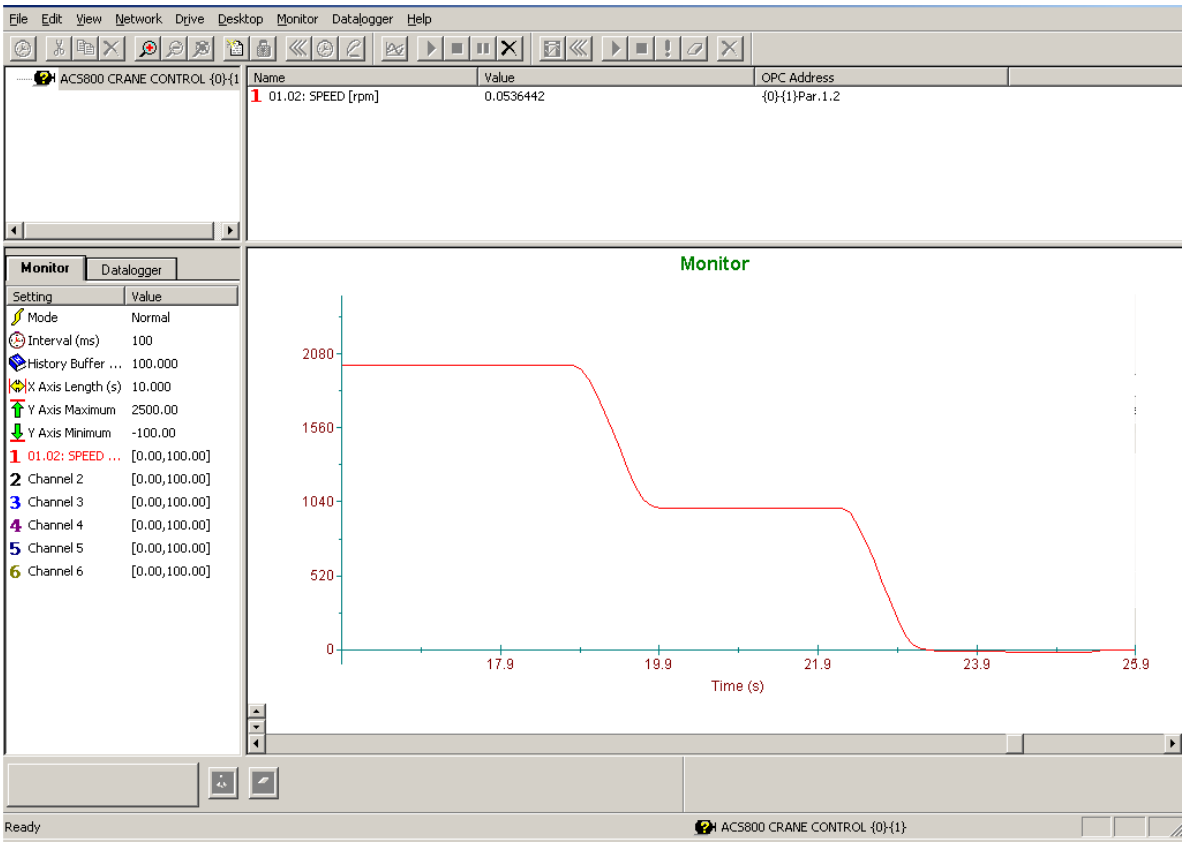

Figure 37.ABB ACS800 ramping-down.

The same principle is applied to ramp down / decelerate crane. After ramping up period (from 0 to t_3), all the oscillation is eliminated during constant speed period (from t_3 to t_4). Therefore, the situation right before t_4 is:

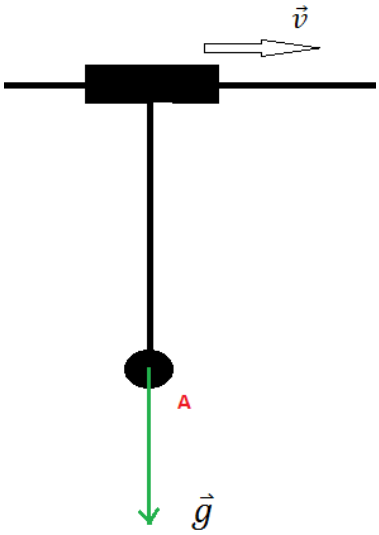

Figure 38. Crane with no oscillation before deceleration period.

Right before t_4, the oscillation's equilibrium position is A and there is no oscillation. At t_4, the speed parameter in motor drive is set to half of target speed. It causes the ramping down of motor speed. Because of deceleration $\vec{a}$, the equilibrium position is shifted to B as follow:

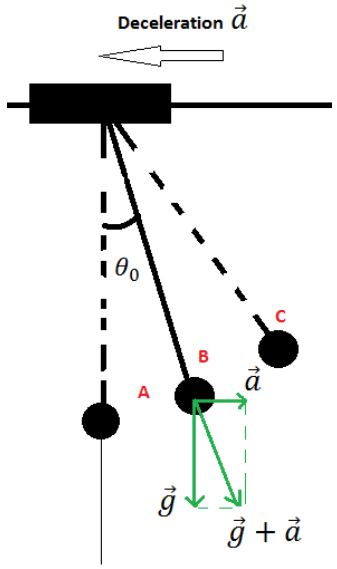

Figure 39. New equilibrium position point B during deceleration.

Because of the shift of equilibrium position, the load starts to oscillate around B with maximum angle (θ_0) at A and C. Suppose that the situation at t_5 is as follow:

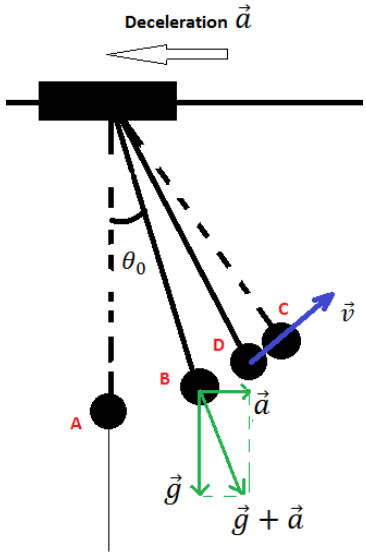

Figure 40. Load is at random position point D during deceleration.

At t_5, the load is at D with certain velocity $\vec{v}$. After t_5, motor is kept at constant speed (half of target speed). As a result, oscillation's equilibrium position is shifted back to A. Algorithm will wait until the load returns back to D with same velocity and in reversed direction as follow:

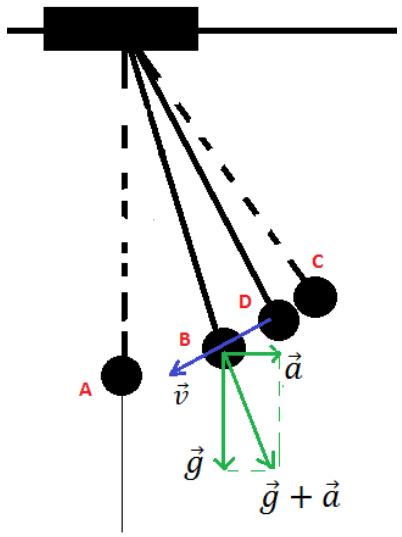

Figure 41. Load is at point D again (in reverse direction).

Right at above situation (t_6), algorithm sets speed parameter in motor drive to 0. The motor, then, will ramp down directly to zero in speed. During t_6 to t_7, the oscillation happens around equilibrium position B, with A as maximum angle.

According to formula, we can derive $(t_5 - t_4) = (t_7 - t_6)$ because we have same deceleration rate and change of speed during these periods. While oscillating around B, it takes $(t_5 - t_4)$ to travel from A→B→D, hence it will also take $(t_7 - t_6)$ to travel from D→B→A. As a result, at t_7 , the load is exactly at A (maximum angle position) with zero velocity, $v_A = 0$. After t_7 , the crane is stopped and no more oscillation is generated anymore. In other words, crane stops stably with no oscillation.

3.4. Anti-sway algorithm pseudo implementation

Let's denote that:

- $a(t_x)$ is swing direction at time t_x. $a(t_x)$ can either be 1 (swing in positive direction) or -1(swing in negative direction).
- $\theta(t_x)$ is vertical angle of the load at time t_x.
- $v(t_x)$ is crane's velocity at time t_x.
- v_{max} is crane's target speed.

The algorithm's logic is presented step by step as follow:

- At t = 0, the algorithm will set motor's speed reference to $\frac{v_{max}}{2}$ and start motor. Motor will ramp up.
- The algorithm will constantly poll actual speed value from motor drive. When actual speed reaches $\frac{v_{max}}{2}$, this moment is t_1. It means $v(t_1) = \frac{v_{max}}{2}$. Algorithm reads $a(t_1), \theta(t_1)$ from inclination sensor.
- The algorithm will constantly poll $a(t), \theta(t)$ until following two conditions is satisfied :
  - $a(t) * a(t_1) < 0$. This formula means the load is moving in opposite direction with $a(t_1)$.
  - $a(t) * \theta(t) + a(t_1) * \theta(t_1) < -\varepsilon, with\ \varepsilon\ is\ a\ very\ small\ number.$ This formula means the load is approaching $\theta(t_1)$ with very small difference ε or the load has already moved past $\theta(t_1)$.

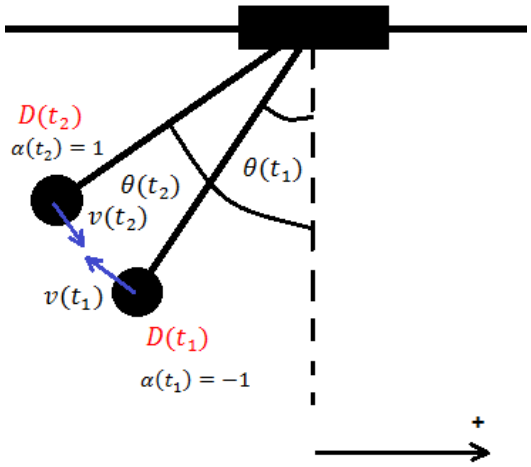

Figure 42. Crane oscillation variables.

If above two formulas are satisfied, the moment is t_2. The algorithm will set speed reference in motor drive to v_{max} causing motor to ramp up to full target speed.

- The algorithm waits until crane's operator presses button to stop the crane (t_4).
- At $t = t_4$, the algorithm will set motor's speed reference to $\frac{v_{max}}{2}$. Motor will ramp down from full speed v_{max} .
- The algorithm will constantly poll actual speed value from motor drive. When actual speed reaches $\frac{v_{max}}{2}$, this moment is t_5. It means $v(t_5) = \frac{v_{max}}{2}$. Algorithm reads $\alpha(t_5), \theta(t_5)$ from inclination sensor.
- The algorithm will constantly poll $\alpha(t), \theta(t)$ until following two conditions is satisfied :
  - $\alpha(t) * \alpha(t_5) < 0$. This formula means the load is moving in opposite direction with $\alpha(t_5)$.
  - $\alpha(t) * \theta(t) + \alpha(t_5) * \theta(t_5) < -\varepsilon, with\ \varepsilon\ is\ a\ very\ small\ number.$ This formula means the load is approaching $\theta(t_5)$ with very small difference ε or the load has already moved past $\theta(t_5)$. Notice that this formula is exactly same as the formula for ramping up period.

- If above two formulas are satisfied, the moment is t_6. The algorithm will set speed reference in motor drive to 0 causing motor to ramp down to zero speed.

3.5. Conclusion

In this chapter, physics model of crane has been introduced and analyzed. Crane's hoist was chosen as observational frame of reference. Based on selected frame of reference, a detailed explanation of swinging phenomenon was presented. In normal crane's operation, swinging of crane is amplified during all periods of crane's movement: ramping up, constant speed and ramping down. In order to minimize swaying of crane, anti-sway algorithm was developed and proven using theoretical physics laws. Motor drive's parameters and inclination sensor's values are served as inputs for anti-sway algorithm. In next chapter, simulation tool will be used to simulate algorithm's behaviors as well as its effectiveness.

4. ANTI-SWAY ALGORITHM SIMULATION

4.1. Introduction

After drafting anti-sway algorithm on paper, there is a need to simulate the algorithm in order to study its behaviors and prove its effectiveness. Some of the most robust physics frameworks have been evaluated including Bullet Physics Library, ODE (Open Dynamics Engine), Newton Game Dynamics and Box2D. Finally, Box2D has been chosen as a simulation framework to examine the performance of the algorithm.

The advantages of Box2D include:

- Using portable C++.
- Modern software design and algorithm.
- Large community support.
- Proven effectiveness through various games such as Angry Birds, Caelum, Crayon Physics, iPhysics, etc.
- Having a good test-bed to support writing experimental models.

In fact, the Box2D engine is so good that it became de facto standard for 2D graphic games nowadays. It has been ported to various languages such as .NET, Java, JavaScript, Flash, etc.

4.2. Simulation model

4.2.1. Simulation model configuration

In order to simulate crane's physics model in Box2D, following Box2D model is used.

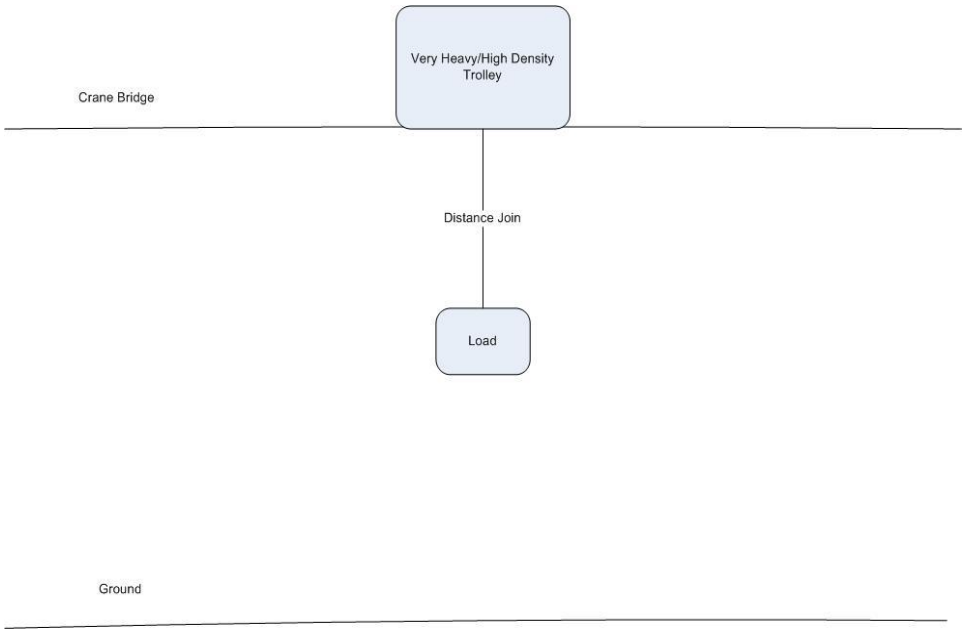

Figure 43. Box2D Physics model.

Box2D model consists of:

- A very long crane bridge with no friction. In reality, the friction with crane's bridge is compensated by motor drive. Therefore, we are not considering friction in this simulation.
- A very heavy trolley so that the sway of load doesn't affect the movement of trolley. This is same as crane's behavior where the motor drive keeps the trolley moving steadily regardless of swinging load. Oscillation of the load will have very little impact on the trolley velocity thanks to mechanical binding between the trolley and the bridge. Moreover, modern motor drive's torque control technology also contributes in reducing effect of load swinging on the trolley
- A load.
- A distance join between load and trolley.

The final Box2D model is built as follow

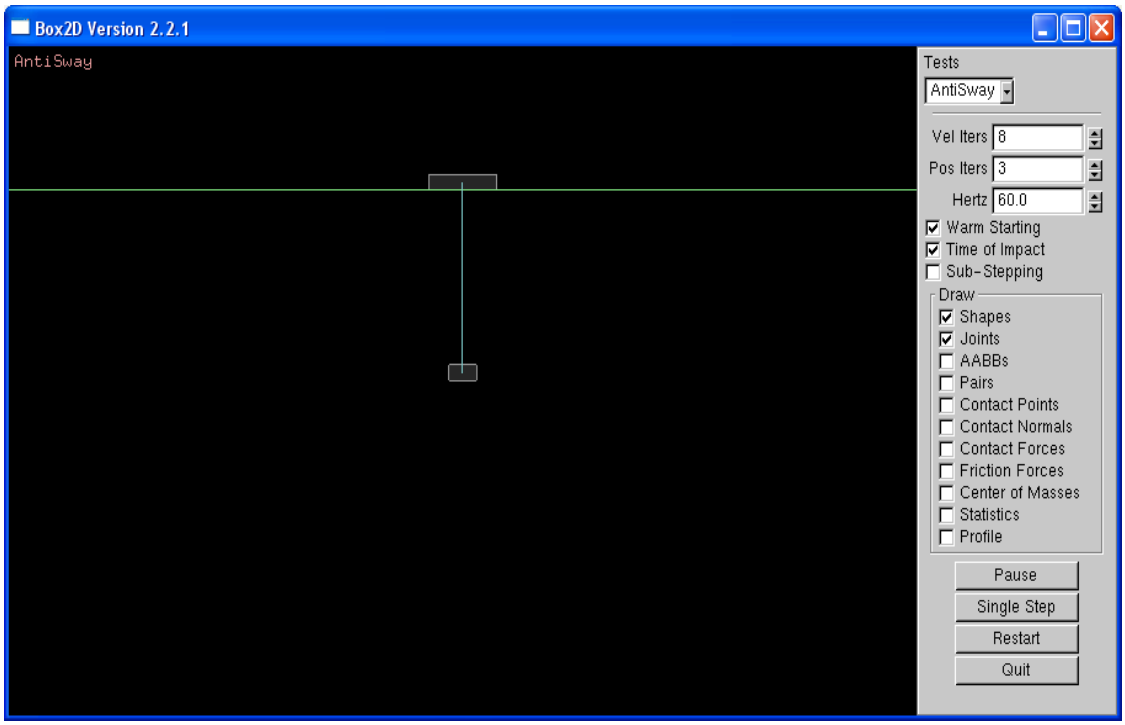

Figure 44. Crane model in Box2D.

By using above settings, different periods during crane's movement can be simulated as follow:

- Ramping up period : a constant positive force is applied to trolley so that the trolley is accelerated with a constant acceleration
- Constant speed period: when the trolley reaches target speed, the trolley is released from the force and it moves steadily during this period.
- Ramping down period: a constant negative force is applied to trolley until it stops.

The Box2D is constructed with parameters defined as in following figure

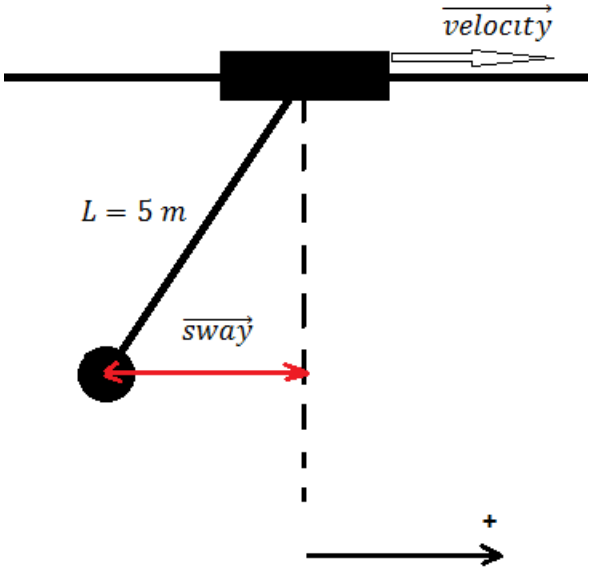

Figure 45. Box2D sample model of crane.

4.2.2. Without anti-sway algorithm simulation results

In case of normal operation (without anti-sway algorithm), the results of simulation are as follow

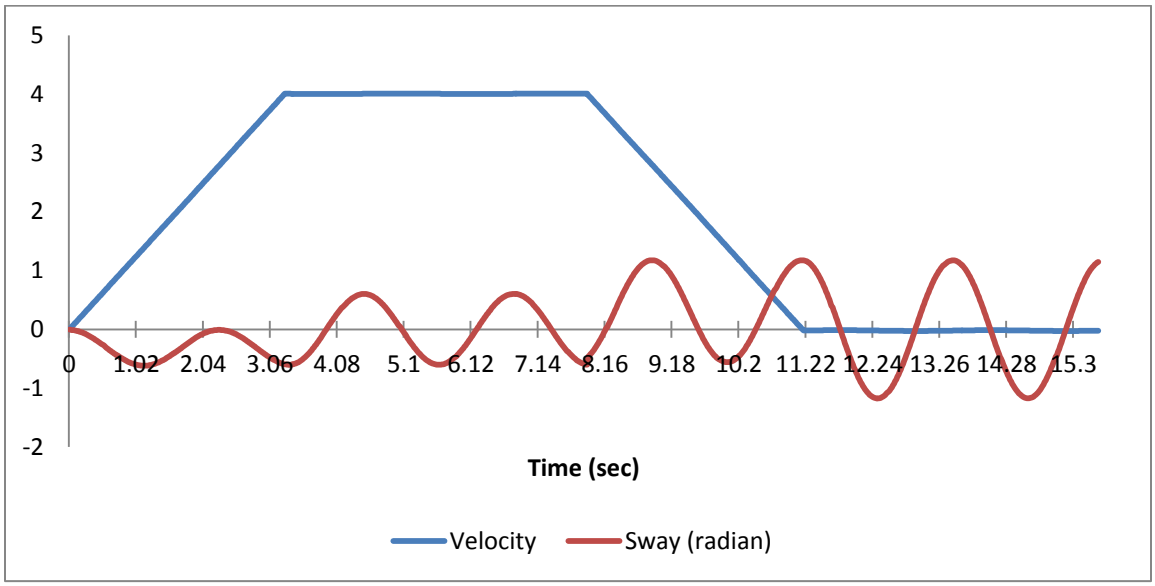

Figure 46. Simulated result in Box2D without anti-sway algorithm (1).

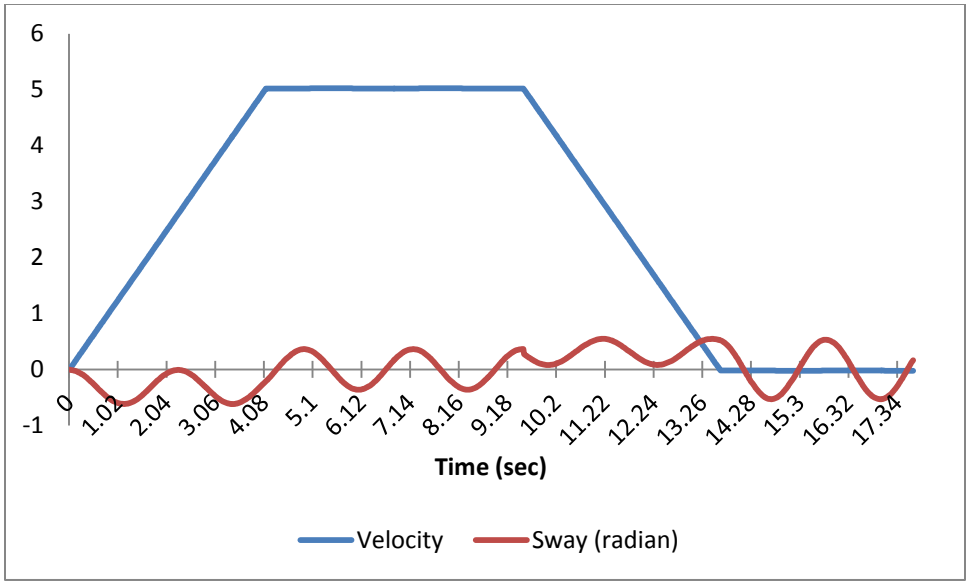

Figure 47. Simulated result in Box2D without anti-sway algorithm (2).

The sway matches well with our theory in 2.4:

- During ramp up period: Sway only happens in negative side.
- During constant speed period: Sway happens symmetrically in both negative and positive sides. Sway's magnitude is amplified in comparison with ramping up period.
- During ramping down: Sway happens much greater in positive side. Sway's magnitude is amplified in comparison with prior periods.
- Stop: Sway happens symmetrically in both negative and positive sides. Sway's magnitude is amplified in comparison with prior periods.

4.2.3. With anti-sway algorithm simulation results

The simulation results with the usage of anti-sway algorithm are as follow

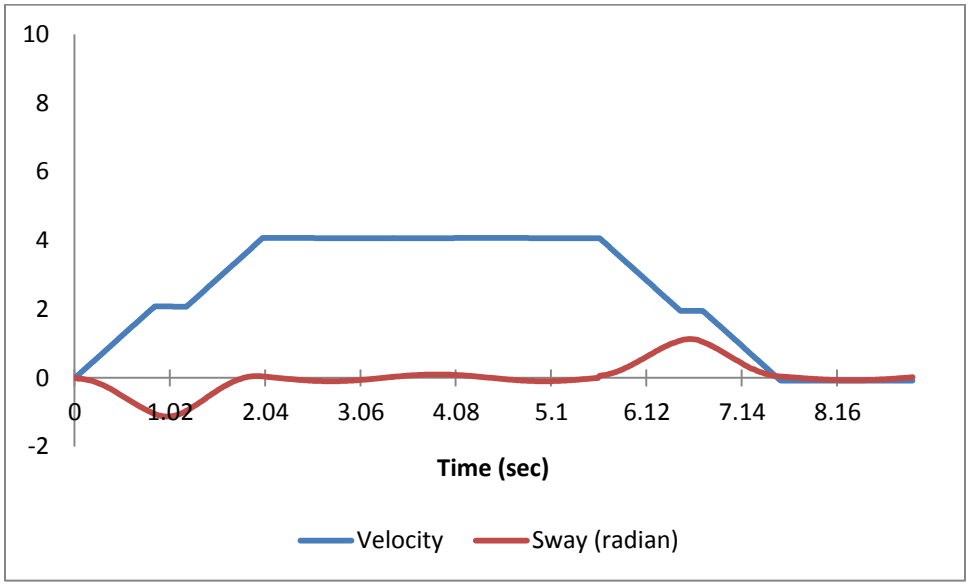

Figure 48. Simulated result in Box2D with anti-sway algorithm (1).

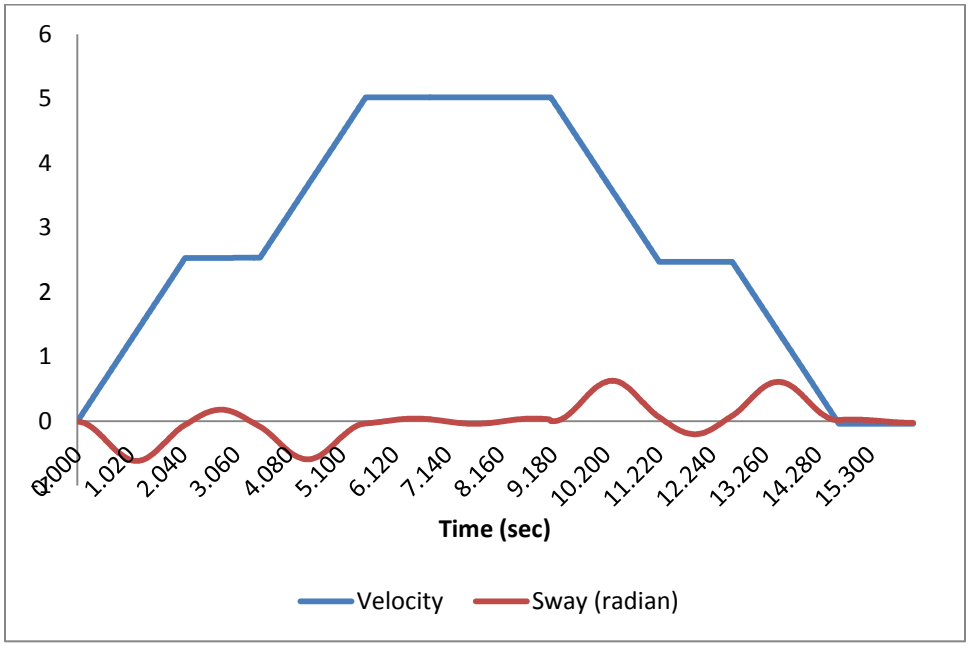

Figure 49. Simulated result in Box2D with anti-sway algorithm (2).

From above simulation result charts, the effectiveness of anti-sway algorithm has been clearly displayed. The sway only happens during ramping up and down periods. During constant speed and fully stop periods, the sway is minimized to almost zero.

4.3. Conclusion

In this chapter, Box2D physics engine is utilized to simulate crane behaviors during normal operation (without anti-sway algorithm) and enhanced operation (with anti-sway algorithm). Theories in chapter 2 and 3 have been proven to be correct and effective in killing load sway during crane movement. With the usage of anti-sway algorithm, the sway is minimized to almost zero during constant speed and full stop period.

5. ABB ACS800 MOTOR DRIVE AND MODBUS PROTOCOL

5.1. Introduction to ABB ACS800 motor drive

Based on theoretical foundation built in previous sections of this paper, the prototype is planned to test the concept of anti-sway on a real crane. Motor drive is a device used variable-frequency technique to control the speed of AC motors. The ABB ACS800 motor drive was selected as the target to test the concept because of its availability. We have a test rack of ACS800 for testing in the laboratory and a real crane controlled by ACS800 in a construction material factory which we can borrow during summer vacation period.

Figure 50. ACS800 test rack

In Figure 43, area marked with number 1 is the ABB ACS800 motor drive. Area marked with number 2 is control board with digital and analog IOs. Lastly, area marked with number 3 is the motor to be controlled.

ABB Group (www.abb.com) is the largest and most innovative motor drive manufacturer nowadays. ABB provides customers with scalable motor control in all ranges of application. ABB drives are bundled with advanced drive technologies and algorithms. Moreover, ABB drive can be extended with optional module such as RTAC (Pulse Encoder Interface Module), RMBA (Modbus Adapter Module), RDCO (DDCS Communication Option Modules)…

The ACS800 Single Drive which belongs to the High Performance Drives group will be our target of implementation and analysis. The ACS-800 includes Start-up Assistant, Adaptive Programming and DTC-Direct Torque Control. Moreover, it is equipped with an optional module RMBA-01(Modbus Adapter Module) which enables the drive control through Modbus RTU RS-485 protocol.

The ACS800 can be connected to a computer via optical fiber cable, NDPA-02 DDCS/PC Card and DriveWindow software. All motor and motor drive parameters can be seen in DriveWindow software. DriveWindow can be used to read, monitor and set value for parameters. Parameters can be used to completely control all features of motor drive such as: start, stop, set maximum speeds, current speed, ramp-up time, ramp-down time, read digital inputs, etc... More details of these parameters can be found in chapter “Actual signals and parameters” (ABB Group, Firmware Manual ACS800 Standard Control Program 7.x)

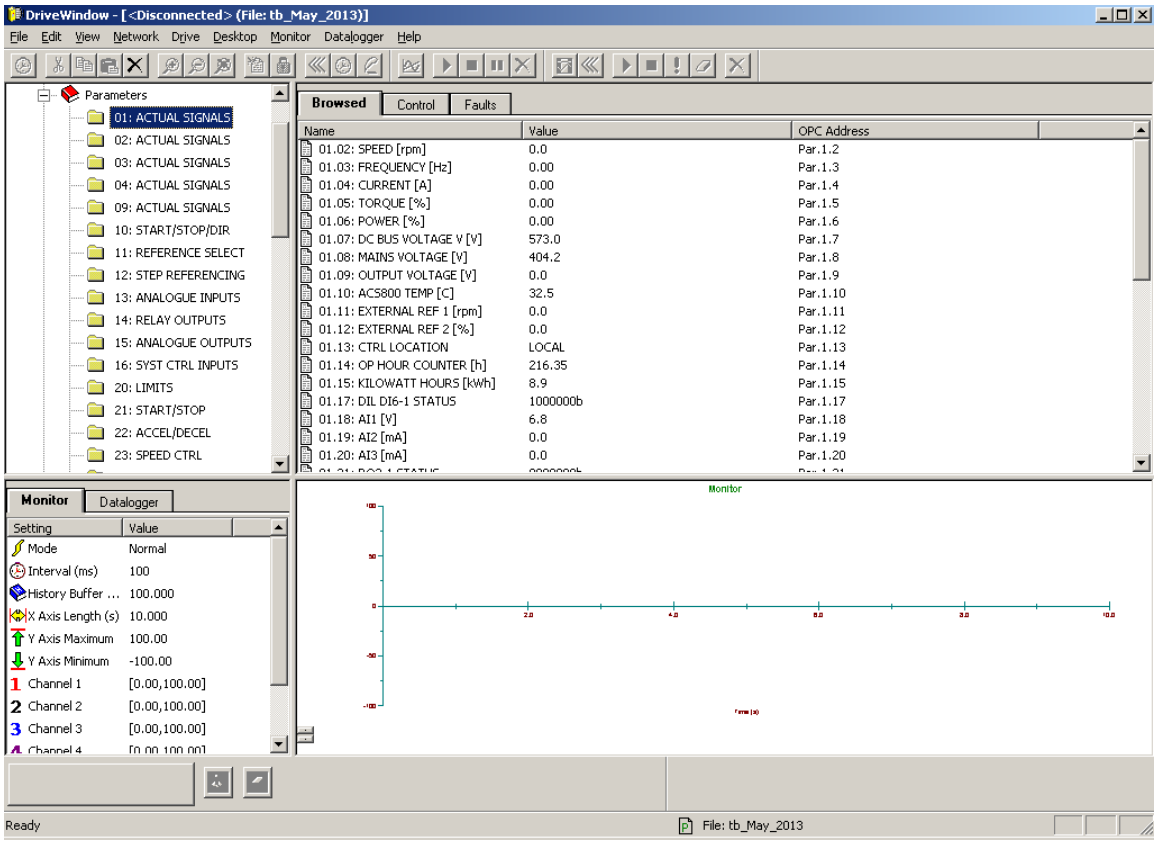

Figure 51. Screenshot of ABB DriveWindow software.

5.2. Introduction to Modbus protocol

Modbus is a serial communication protocol initially developed by Modicon to enable communication with Modicon's programmable logic controller (PLCs). Later in 1979, Modicon published Modbus as open communication protocol. After that, Modbus has been adapted and developed by many industrial equipment producers. Nowadays, it is one of the most popularly supported protocols among industrial electronic devices. Currently, the Modbus Organization is holding the responsibility to develop Modbus standards and provide support worldwide. (http://modbus.org/)

Some of the reasons behind Modbus's popularity are:

- Its focus on industrial applications and devices.
- Open protocol, no licensing fee to use and develop.

- Its simplicity, robustness and vendor-independence.
- Easy deployment: most of the communication channel can implement Modbus protocol, including wireless, twisted pair line, Ethernet, fiber optics...

Modbus employs a master-slaves design over serial communication technique. In a Modbus network, there is only one single master which can communicate with many slaves. The number of slaves in a network can be up to 247 slaves. Every slave has its unique identification number within a network to identify itself. The communication is always initiated by the master; the master can send command/query to slaves to instruct slaves 'actions or acquire measurement values. The slaves only can reply to the master's commands.

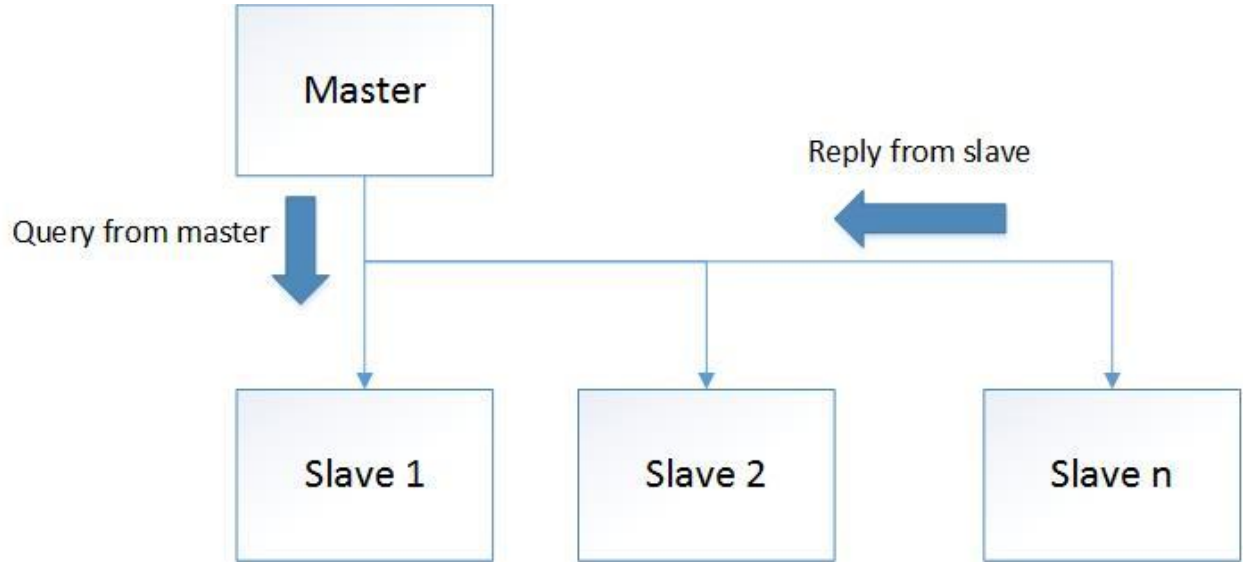

Figure 52. Modbus master-slave communication**.**

Modbus is asynchronous and does not define the physical interface. Popular physical interfaces for Modbus includes RS-232 and RS-485.

Modbus protocol can be enabled for ACS800 by using ABB's RMBA-01 (Modbus Adapter Module). RMBA module only supports Modbus RTU (Remote Terminal Unit) over galvanically-isolated serial RS-485. Therefore, our discussion of Modbus protocol will focus on Modbus RTU over RS-485.

Most important specification details of RMBA-01 module are listed as follow (User's Manual Modbus Adapter Module RMBA-01, 2002:30-31).

- Size of the link: 247 stations including repeaters (31 stations and 1 repeater per segment).
- Medium: Shielded, twisted pair RS485 cable.
- Termination: built in, active type.
- Maximum Bus Length: 1200 m.
- Topology: Multi-drop.
- Serial communication type: Asynchronous, half duplex.
- Transfer rate: 600, 1200, 2400, 4800, 9600, 19200 bit/s.
- Protocol: Modbus RTU.

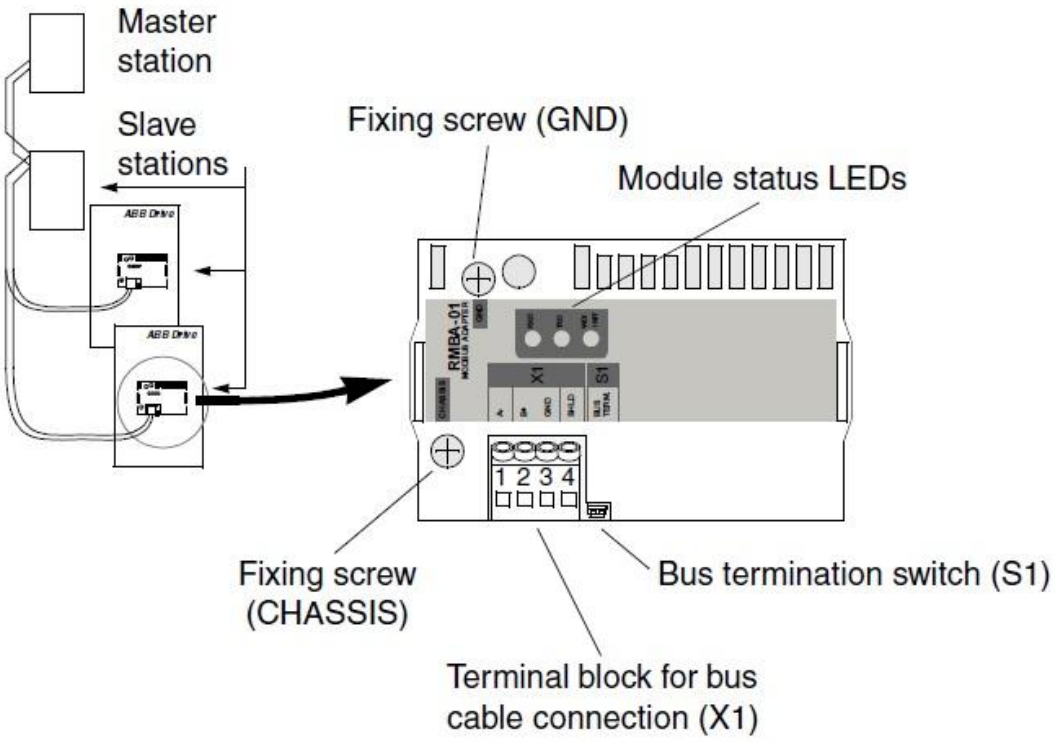

Figure 53. RMBA-01 module layout (ABB Group, 2002:14. *User's Manual Modbus Adapter Module RMBA-01*).

Figure 54. Modbus Adapter Module installed on ACS800's control panel (area marked in red rectangular).

Within the scope of anti-sway application, not all functions of Modbus are used. Only two following functions of Modbus are used and implemented:

- Function number 3: Read Holding Registers. This function is used to read multiple consecutive parameters from the drive.
- Function number 16: Preset Multiple Registers. This function is used to write multiple consecutive parameters to the drive.

5.2.1. Modbus function number 3 (Read Holding Registers)

Modbus RTU works only with 2 byte parameters. Therefore, after read holding register query is sent successfully from Modbus master, the corresponding slave will send back values of requested parameters using 2 byte format.

Query frame format

Table 1. Modbus function number 3 query frame.

Name	Length	Function
Start	3.5 characters idle	At least 3,5 character times of silence
Address	8 bits	Slave address
Function	8 bits	Function code(in this case 0x03)
Register address	16 bits	The data address of the first register requested starts from 40001.
Register count	16 bits	The total number of registers requested.
CRC	16 bits	The CRC (cyclic redundancy check)
End	3.5 characters idle	At least 3,5 character times of silence

Reply frame format

Table 2. Modbus function number 3 reply frame.

Name	Length	Function
Start	3.5 characters idle	At least 3,5 character times of silence
Address	8 bits	Slave address
Function	8 bits	Function code(in this case 0x03)
Data byte count	8 bits	The number of data bytes to follow

Register values	Length is the value of data byte count.	Values of requested parameters. 2 bytes/ parameter.
CRC	16 bits	The CRC (cyclic redundancy check)
End	3.5 characters idle	At least 3,5 character times of silence

5.2.2. Modbus function number 16 (Preset Multiple Registers)

The Modbus master will request slave to change its parameter values by using function number 16 (Preset multiple registers). Parameter value is represented as 2 bytes per each.

Query frame format

Table 3. Modbus function number 16 query frame.

Name	Length	Function
Start	3.5 characters idle	At least 3,5 character times of silence
Address	8 bits	Slave address
Function	8 bits	Function code(in this case 0x10)
Register address	16 bits	The data address of the first register starts from 40001.
Register count	16 bits	The number of registers to write.
Data byte count	8 bits	The number of data bytes to follow
Register values	Length is the value of data byte count.	Values of parameters to write. 2 bytes/ parameter.

CRC	16 bits	The CRC (cyclic redundancy check)
End	3.5 characters idle	At least 3,5 character times of silence

Reply frame format

Table 4. Modbus function number 16 query frame.

Name	Length	Function
Start	3.5 characters idle	At least 3,5 character times of silence
Address	8 bits	Slave address
Function	8 bits	Function code(in this case 0x10)
Register address	16 bits	The data address of the first register starts from 40001.
Register count	16 bits	The number of registers written.
CRC	16 bits	The CRC (cyclic redundancy check)
End	3.5 characters idle	At least 3,5 character times of silence

5.3. Modbus configuration for ACS800

In order to enable RMBA to control ACS800 using EXT1(external 1) channel, following parameters need to be modified from DriveWindow:

Table 5. Modbus configuration for ABB ACS800.

Parameter code	Parameter name	Parameter description	Value	Value Description

10.01	EXT1 STRT/STP/DIR	Defines the connections and the source of the start, stop and direction commands for external control location 1 (EXT1).	COMM.CW	Fieldbus Control Word.
10.03	REF DIRECTION	Enables the control of rotation direction of the motor, or fixes the direction.	REQUEST	Direction of rotation control allowed
11.02	EXT1/EXT2 SELECT	Defines the source from which the drive reads the signal that selects between the two external control locations, EXT1 or EXT2.	EXT1	EXT1 active
11.03	EXT REF1 SELECT	Selects the signal source for external reference REF1	COMM. REF	Fieldbus reference REF1
12.01	CONST SPEED SEL	Activates the constant speeds or selects the activation signal.	NOT SEL	No constant speeds in use
30.18	COMM FLT FUNC	Selects how the drive reacts in a fieldbus communication	NO	Protection is inactive.

		break, i.e. when the drive fails to receive the Main Reference Data Set or the Auxiliary Reference Data Set.		
16.01	RUN ENABLE	Sets the Run Enable signal on, or selects a source for the external Run Enable signal. If Run Enable signal is switched off, the drive will not start or stops if it is running	YES	Run Enable signal is on.
52.01	STATION NUMBER	Defines the address of the device. Two units with the same address are not allowed on-line.	1	Currently, only one drive is supported by anti-sway master device
52.02	BAUDRATE	Defines the transfer rate of the link.	19200	19200 bit/s
52.03	PARITY	Defines the use of parity and stop bit(s). The same setting must be used in all on-line stations.	NONE1STOPBIT	No parity bit, one stop bit

98.02	COMM. MODULE LINK	Activates the external serial communication and selects the interface	STD MODBUS	The drive communicates with a Modbus controller via the Modbus Adapter Module (RMBA) in option slot 1 of the drive

More details of ACS800's parameters can be found in chapter "Actual signals and parameters" (ABB Group, Firmware Manual ACS800 Standard Control Program 7.x)

5.4. Conclusion

The ABB ACS800 motor drive is chosen as our first target to verify the concept of anti-sway on a crane. Moreover, among many others, Modbus was selected as a standard communication protocol to communicate between anti-sway device and motor drive. Modbus is a ubiquitous protocol for industrial devices. Thus, anti-sway device has ability to extend support to other vendors such as: Vacon, Kone, etc.

Among many Modbus's functions, function number 16 (Preset multiple registers) and function number 3 (Read Holding Registers) are presented in details. The anti-sway device will utilize these Modbus functions to communicate with motor drives. Modbus configuration for ACS800 is also demonstrated in this chapter.

Via Modbus protocol, it is possible to:

- Send commands to the drive (Stop, Run, Run Enable, etc).
- Set motor speed or torque reference.
- Read motor's status and actual measurement values from the drive.
- Read/set parameters.

- Reset fault.

Above possibilities allow us to implement anti-sway solution for ABB ACS800 motor drive.

6. ARCHITECTURE OF ANTI-SWAY DEVICE

6.1. Introduction

In this section, the architecture overview of anti-sway device will be presented. Moreover, connections between different parts of the system are illustrated. As a result, readers will have a broad picture of how the final device will look like after going through this chapter.

6.2. Architecture and connection diagrams

A minimal anti-sway device will consist of following hardware components:

- A central MCU (Microcontroller Unit) that run anti-sway algorithm and communicate with motor drive via Modbus.
- A RS-485 transceiver to receive and transmit Modbus RS-485 signal.
- An inclination sensor mounted to crane's rope to measure the angle. The inclination sensor is mounted to the static part of the crane ropes.

Separated software modules are also required:

- Modbus driver: to communicate from MCU and motor drive.
- Anti-sway algorithm as presented in chapter 3 of this paper.
- Kalman filter to smoothen and correct measurement from inclination sensor.

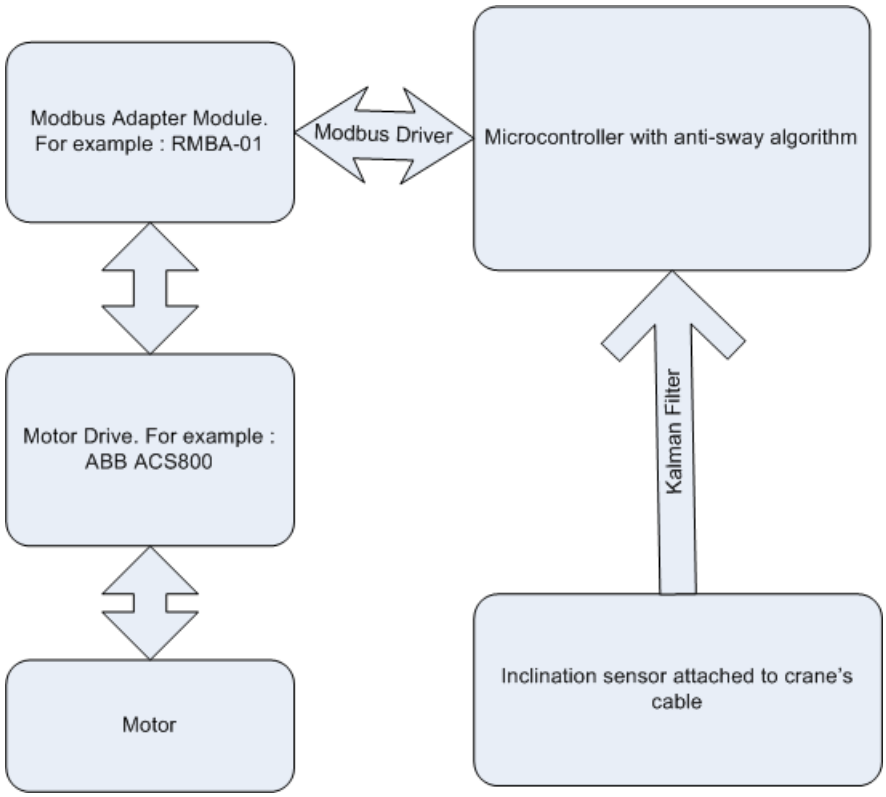

Figure 55. Block diagram of anti-sway device.

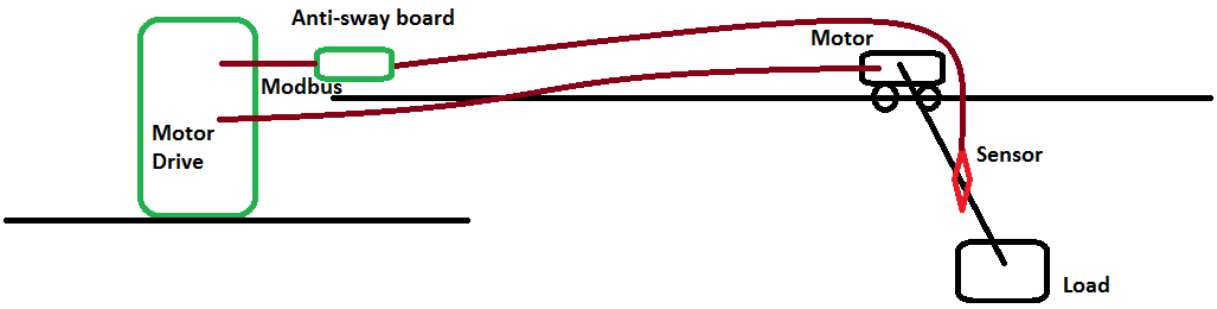

Figure 56. System connections.

Figure 57. Static part of crane's rope.

The inclination sensor must be attached to the static part of the crane.

6.3. Conclusion

The block and connection diagrams have been demonstrated within this chapter. Generally, for a minimal anti-sway device, three essential hardware parts are required: central MCU, RS-485 transceiver and inclination sensor. Similarly, three separate software modules are also required: Modbus driver, anti-sway algorithm and Kalman filter. With the combination of software and hardware parts, anti-sway prototype device will be built and tested in coming chapters.

7. FIRST GENERATION PROTOTYPE WITH ARDUINO BOARD

7.1. Introduction

This is a very early prototype implementation of the device. The main purpose is to verify the concept of anti-sway algorithm before developing any further. The microcontroller will be the central processing unit which contains the anti-sway algorithm and communicate with motor drive via Modbus and acquiring measurement data from inclination sensor. We started with an Arduino Duemilanove board which is very inexpensive, fast and easy to build the prototype.

7.2. Arduino Duemilanove introduction

Arduino is an open-source electronics prototyping platform. Arduino Duemilanove is a microcontroller board based on ATmega168 or ATmega328. The hardware is packed with following capacity:

- 14 digital input/output pins (of which 6 can be used as PWM outputs).
- 6 analog inputs.
- 16 MHz crystal oscillator.
- A USB connection, a power jack, an ICSP (In-circuit serial programming) header, and a reset button.

Table 6. Arduino Duemilanove features.

Microcontroller	ATmega168
Operating Voltage	5V
Input Voltage (recommended)	7-12V
Input Voltage (limits)	6-20V
Digital I/O Pins	14 (of which 6 provide PWM output)

Analog Input Pins	6
DC Current per I/O Pin	40 mA
DC Current for 3.3V Pin	50 mA
Flash Memory	16 KB (ATmega168) or 32 KB (ATmega328) of which 2 KB used by bootloader.
SRAM	1 KB (ATmega168) or 2 KB (ATmega328)
EEPROM	512 bytes (ATmega168) or 1 KB (ATmega328)
Clock Speed	16 MHz

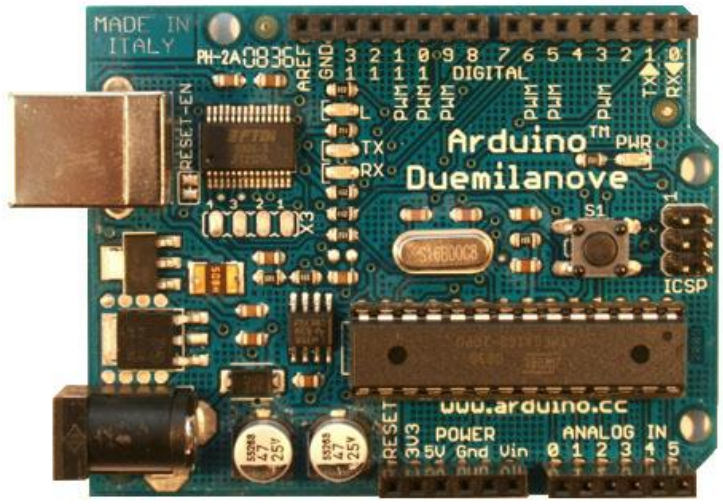

Figure 58. Arduino Duemilanove.

Arduino board is also shipped with standard IDE (Integrated Development Environment) based on Wiring (http://wiring.org.co/). Arduino developer can write AVR code in a C/C++-derived language called Wiring. Therefore, the algorithm code which was used in Box2D simulation environment can be quickly ported to Arduino.

7.3. ASM PTAM27 inclination sensor introduction

The selected inclination sensor for this first generation prototype is ASM PTAM27-1-180-U6-CW-T0.1-KAB2M produced by ASM - Automation, Sensors, and Measurement GmbH (http://www.asm-sensor.com/). The sensor provides linear analog output, wear free, high resolution, small delay and high shock resistance capabilities.

Most important properties of this sensor are listed in following table.

Table 7. ASM PTAM27 features.

Property name	Property value	Description
Protection class	IP67	• Totally protected against dust. • Protected against the effect of immersion between 15cm and 1m.
Output/Excitation	U6	Voltage 0.5 ... 4.5 V / UB = 5 V DC ±5%
Number of axes	1	Inclination in X axis (mounting X)
Measurement range	±1°... ±180° in 1° increments	
Resolution	0.1°	
Linearity	1 axis : ±0.5° (≤±75°), ±1° (>7±5°)	
Material	Plastic	
Connection	KAB2M	Cable 5 x 0.25 mm2, standard length 2 m
Characteristic	CW	Increasing signal for CW (clock-wise) inclination
Output delay	T0.1	Delay 0.1 second
Shock (non-operational)	EN60068-2-27:1993	100 g/11 ms, 100 shocks
Vibration (non-operational)	EN60068-2-6:1995	20 g/10 Hz-2 kHz, 10 cycles

Figure 59. PTAM27 inclination sensor (**ASM GmbH**, 2012. *PTAM27 Universal MEMS Inclination Sensor with Analog Output*).

According to the specification, this is one of the best inclination analog sensors available at present. More details of ASM PTAM27 sensor can be found in "PTAM27 Universal MEMS Inclination Sensor with Analog Output" (ASM GmbH, 2012).

7.4. Kalman filter for inclination sensor

7.4.1. Introduction

With the usage of inclination sensor, it is required to have Kalman filter to address noisy measurements. The noisy data is fed to Kalman filter and less noisy data is returned by Kalman algorithm.

"The Kalman filter is a set of mathematical equations that provides an efficient computational (recursive) means to estimate the state of a process, in a way that minimizes the mean of the squared error. The filter is very powerful in several aspects: it supports estimations of past, present, and even future states, and it can do so even when the precise nature of the modeled system is unknown." (G. Welch and G. Bishop, 2004).

Our process can be considered similar as sloshing in which the measurement is oscillating in form of sin wave. This is a non linear process which normally requires using extended Kalman filter to model the process correctly. However, in this prototype, we can avoid the complexity and slowness of extended Kalman filter in embedded system by relaxing original Kalman model.

7.4.2. Kalman filter formulas

Discrete Kalman formulas are represented as follows:

Predict

$$\hat{x}_k^- = F_k * \hat{x}_{k-1} + B_k * u_k \quad (7.1)$$

$$P_k^- = F_k P_{k-1} F_k^T + Q \quad (7.2)$$

Update

$$K_k = P_k^- H^T (H P_k^- H^T + R)^{-1} \quad (7.3)$$

$$\hat{x}_k = \hat{x}_k^- + K_k (z_k - H_k \hat{x}_k^-) \quad (7.4)$$

$$P_k = (I - K_k H) P_k^- \quad (7.5)$$

Where

$\hat{x} : Estimated\ state.$

$F : State\ transition\ matrix.$

$u : Control\ variable.$

$B : Control\ matrix.$

$P : State\ variance\ matrix.$

$Q : Process\ variant\ matrix\ .$

$z : Measurement\ variable.$

$H : Measurement\ matrix.$

$K : Kalman\ gain.$

$R :\ Measurement\ variance\ matrix.$

Subscripts are as follows: k current step, k – 1 previous step.

Superscript is as follows: '–' is intermediate step.

(Greg Welch and Gary Bishop, 2006).

7.4.3. Kalman model for anti-sway process

A simple 2–D Kalman filter is implemented to correct noisy angle measurement from inclination sensor. Our relaxed model is built as follow (constant-velocity particle model):

$$\alpha_t = \alpha_{t-1} + \dot{\alpha} * \Delta t$$

Where

α_t and α_{t-1} are sway angle at time t and $t - 1$ respectively.

$\dot{\alpha}$ is angular velocity ($\dot{\alpha} = \frac{d(\alpha)}{dt}$).

As a result, the continuous state-space equations are as follow:

$$\dot{x}(t) = Ax(t) + w(t);$$

$$z(t) = Hx(t) + v(t);$$

With $A = \begin{bmatrix} 0 & 1 \\ 0 & 0 \end{bmatrix}$ and $H = [\,1 \quad 0]$

➔ Discrete state transition matrix is $F_k = e^{A\Delta t} = I + \sum_{i=1}^{\infty} \frac{\Delta t^i A^i}{i!} = \begin{bmatrix} 1 & \Delta t \\ 0 & 1 \end{bmatrix}$

$B_k, u_k = 0$. (Control variables are 0).

We cannot measure angular velocity, therefore our measurement is:

$$z = z$$

Where z is the noisy angle measurement from sensor.

We assumed that noise only caused by the swinging motion (angular velocity noise). Therefore, the continuous process variant matrix can be represented as:

$$Q = \begin{bmatrix} 0 & 0 \\ 0 & q \end{bmatrix}$$

As a result, we have the discrete Q matrix (Dah-Jing Jwo, 2007:6):

$$Q_k = q * \begin{bmatrix} \frac{\Delta t^3}{3} & \frac{\Delta t^2}{2} \\ \frac{\Delta t^2}{2} & \Delta t \end{bmatrix}$$

$P_0 = \begin{bmatrix} 1000 & 0 \\ 0 & 1000 \end{bmatrix}$. (Random initial value for state variance).

R=1. (Error 1^o from PTAM27 specification).

$B_k, u_k = 0$. (Control variables are 0).

$q = 0.8$.

$\Delta t = 0.05$. (Sampling rate).

7.4.4. Kalman filter results

The testing results of the Kalman filter are displayed in following graphs.

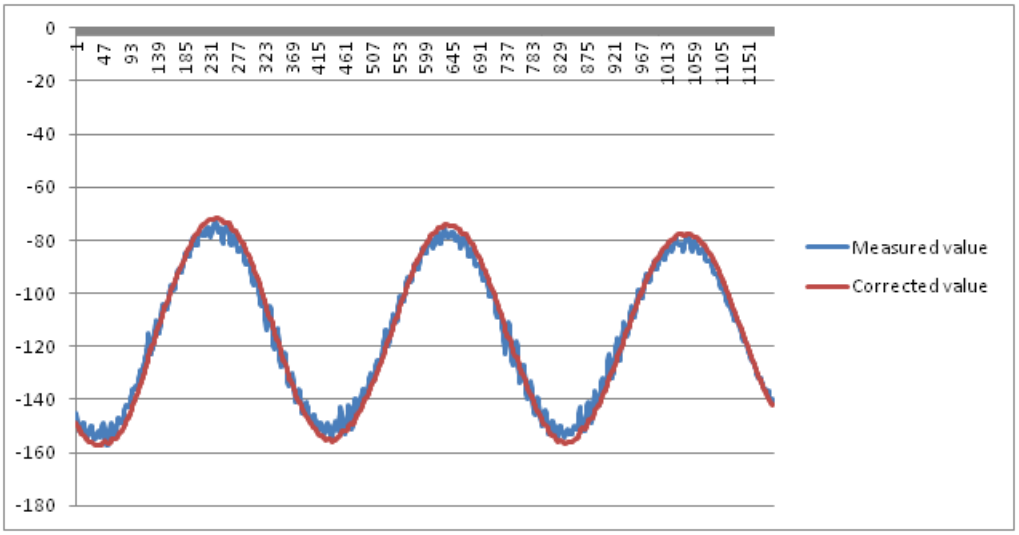

Figure 60. Kalman filter testing result (1).

In the following graph, the swing direction is also displayed in green color. The max level of the green line means swing direction is positive. Otherwise, swing direction is negative.

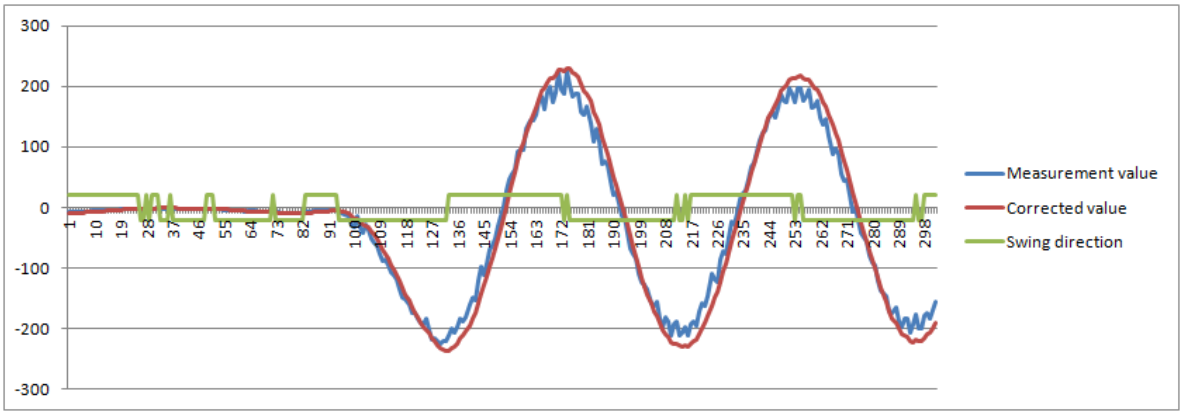

Figure 61. Kalman filter testing result (2).

According to above graphs, it is clearly shown that the noisy measurement values have been smoothened along the way. The implemented Kalman filter is able to detect and correct noises, abnormal jumps in measured values. Moreover, the direction of the swinging is detected more accurately based on corrected values.

However, Kalman filter is based on floating point mathematic operations. According to Loughborough Sound Images (1997), using floating point arithmetic can cause overhead ranges between a factor of 10 and 500 in comparison with fixed-point arithmetic. Since, our Kalman filter will run in fast circle to update and estimate sensor values, floating point arithmetic can potentially hurt performance of the application. Therefore, Kalman filter was improved with the introduction of Q16 fixed-point format to represent floating point numbers.

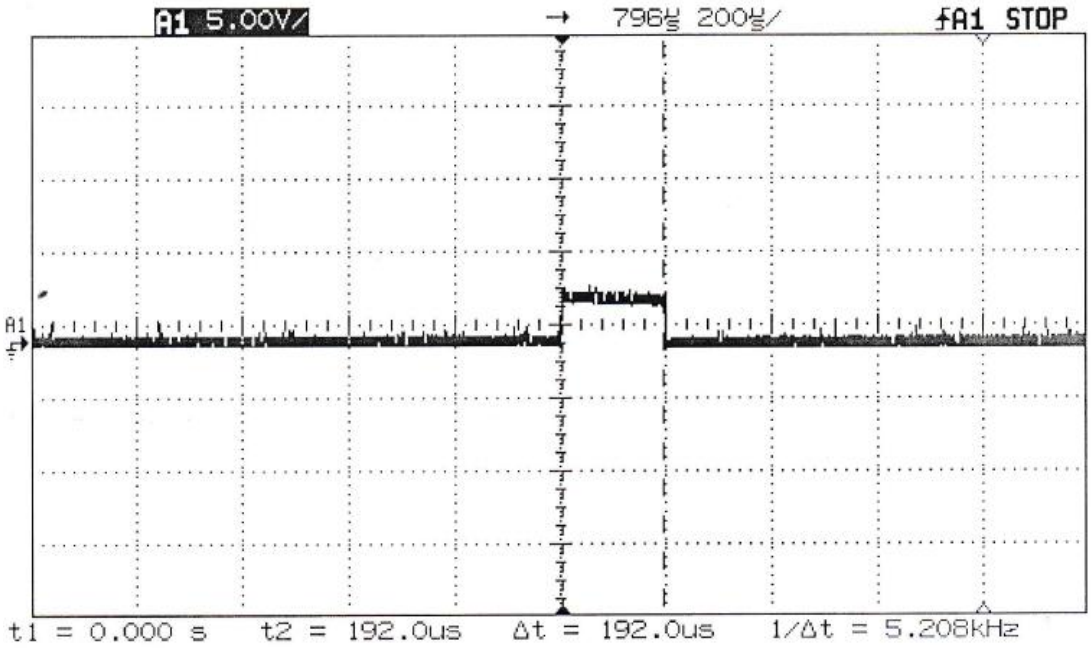

Figure 62. Kalman filter update takes 192 microseconds with floating point arithmetic.

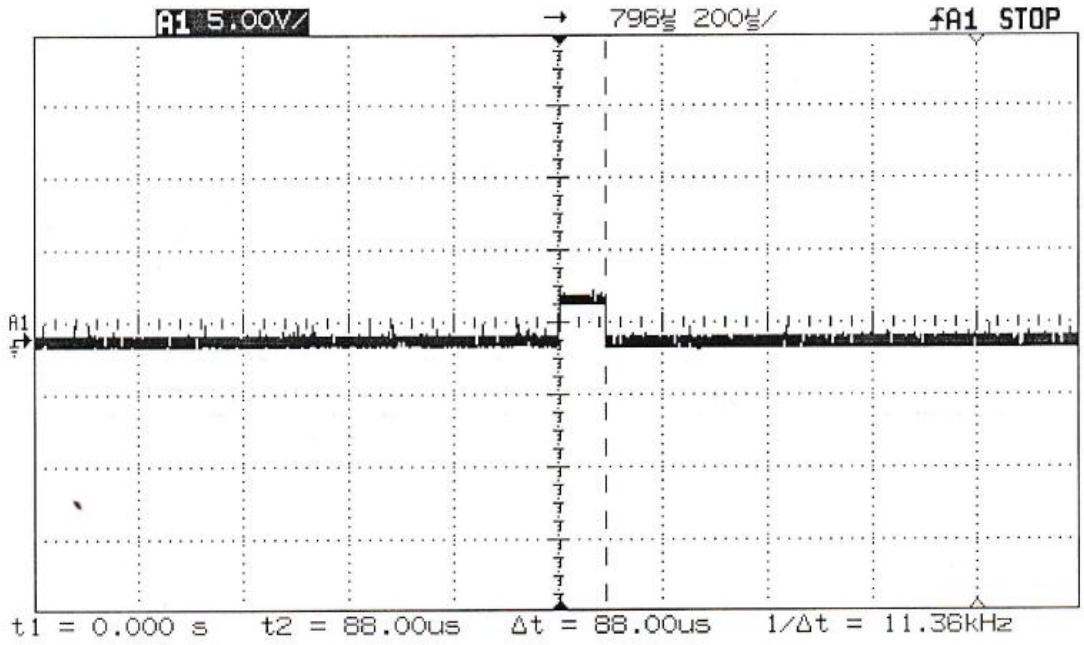

Figure 63. Kalman filter update takes 88 microseconds with Q16 fixed point arithmetic.

As the result, we can see a big improvement in performance of Kalman filter. Time taken with Q16 fixed point algorithm was reduced to less than 43% of floating point algorithm time.

Accurate measurement of angle and direction is top-priority in anti-sway algorithm. Therefore, the successful implementation of fast Kalman filter certainly improves the effectiveness and accuracy of anti-sway algorithm.

7.5. ST485 transceiver

ST485 is a low-power transceiver of RS-485 and RS-422 signals from ST Electronics (http://www.stee.stengg.com/).

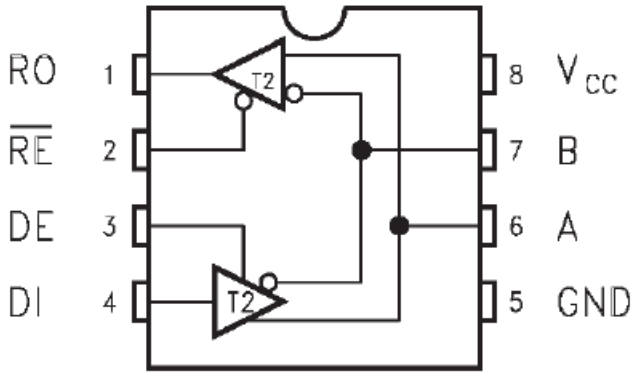

Figure 64. ST485 pin configuration.

Pin description

Table 8. Pin configuration of ST485.

Pin number	Symbol	Name and function
1	RO	Receiver Output
2	$\overline{RE}$	Receiver Output Enable
3	DE	Driver Output Enable
4	DI	Driver Input
5	GND	Ground
6	A	Non-inverting Receiver Input and Non-inverting Driver Output
7	B	Inverting Receiver Input and Inverting Driver Output
8	V_{CC}	Supply Voltage

ST485 employs TTL (Transistor–transistor logic) logic level (5 V ±10%).

7.6. Prototype board

The connection of the prototype looks as follow

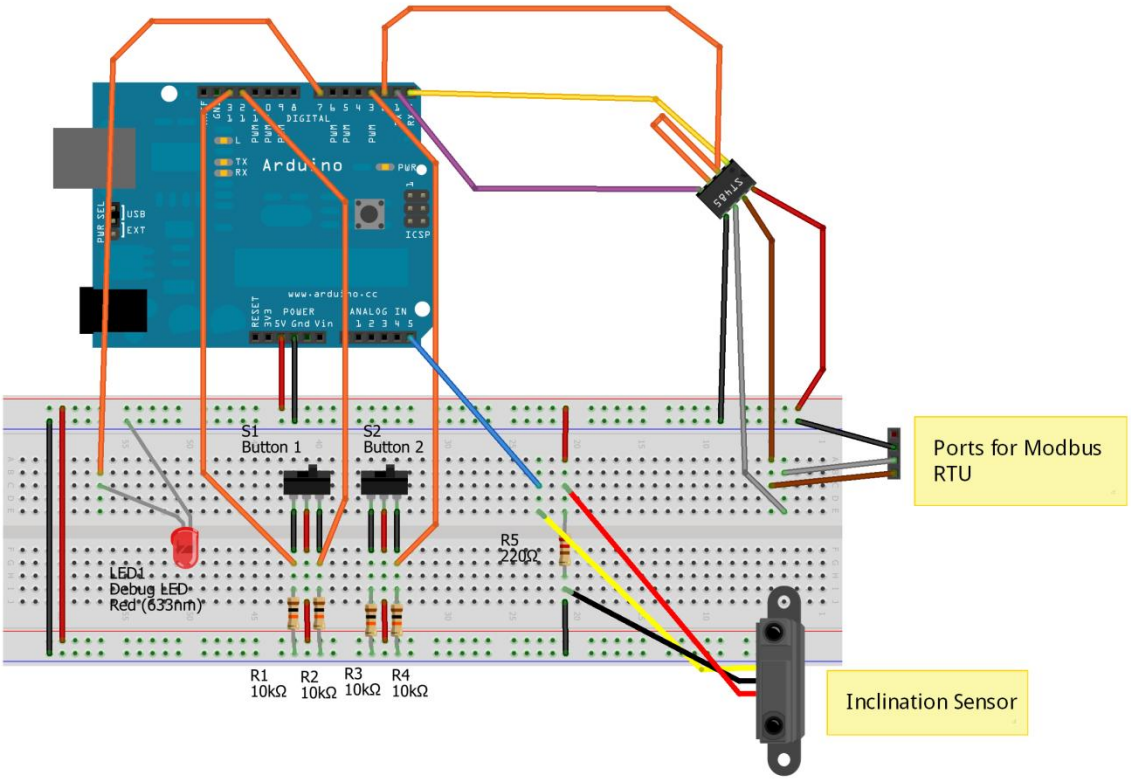

Figure 65. Anti-sway prototype with Arduino.

Prototype design and functionalities:

Button 2 is used to switch on initial communication establishment with the drive. After turning button 1 to ON (switch to the right) for 5 seconds, the motor should be at the READY_TO_GO state. Currently, only right switch of this button is connected.

Button 1 is used to START/STOP the motor. Right switch is used to start the motor. On the other hand, motor stops if the left switch is ON.

R1, R2, R3 and R4 are pull-up resistors for buttons. Typical value for pull-up resister is 10 KOhm.

ST485 chip is used to convert RS485 signal from Modbus RTU of motor drive to UART of Arduino.

R5 is used to reduce the current flowing in the sensor by connecting it in parallel with the sensor. The maximum current of ASM PTAM27-1-180-U6-CW-T0.1-KAB2M is only 20 mA, while the output current of the Arduino is 40mA.

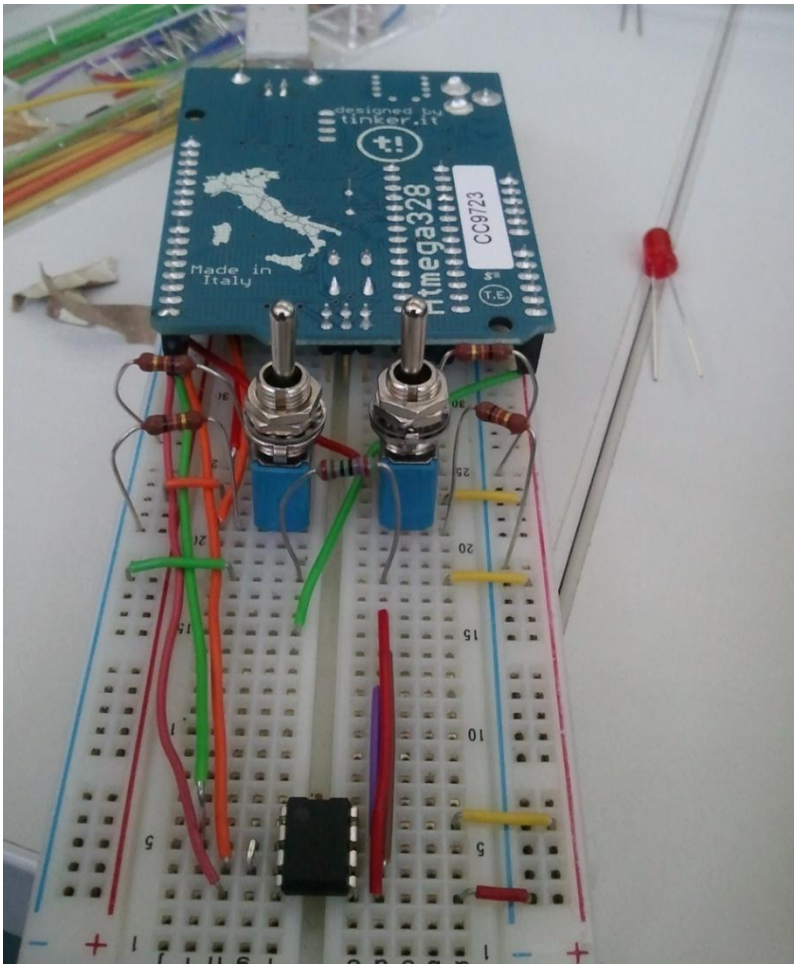

Figure 66. Actual picture of anti-sway Arduino-based prototype.

7.7. Testing results

After the board is set-up and tested against the ACS800 test rack, the board is taken to the factory to test with real ACS800 crane. Inclination sensor is mounted to crane's wire rope

and connected to our Arduino board. Then, our Arduino board is connected to ACS800 via Modbus cable. Although we only managed to borrow the crane and arrange testing session in four days, the final results show really promising result of the described anti-sway algorithm. The board was able to start, stop and modify crane's speed properly. Moreover, the anti-sway algorithm has been able to reduce swinging significantly.

During testing session, some videos have been captured to demonstrate the effectiveness of anti-sway algorithm.

- Video when the operator is operating crane normally(without anti-sway board) https://www.youtube.com/watch?v=T8GPoLyKeX4
- Video when the operator is operating crane with help of anti-sway algorithm https://www.youtube.com/watch?v=JDQ6FlAgZ60

In the video, the crane was carrying a very heavy hook which weights around 1 ton. The anti-sway board was kept on the ground for debugging purposes. Therefore, the crane can only move maximum approximately 20 meter distance because of the connection between the anti-sway board and the inclination sensor.

In the first video where the operator is performing the crane movement normally, the oscillation matches really well with our theory in 2.4. The oscillation always happens and it is amplified during crane's movement. At destination position, the crane swings heavily.

In the second video where the operator is performing the same crane movement via buttons on anti-sway board, the oscillation does not exist during crane movement. The hook travels smoothly when the crane reaches maximum speed. At destination, the crane stops quietly with almost no sway. There was very small sway caused by the rotation of the hook around its gravity center.

7.8. Conclusion

The anti-sway prototype board's hardware is introduced in this chapter. A Kalman filter was also implemented to minimize noise from inclination sensor's measurement. Moreover,

testing results of anti-sway prototype board with real crane are described to prove the efficiency of anti-sway algorithm. The algorithm implementation was capable of minimizing dramatically the sway of crane during its movement.

However, some hardware defects are detected during testing sessions:

- Using TTL analog sensor in factory results in much noise because of electrostatic generated from metals.
- Using TTL analog sensor with long distance cable also results in much noise.
- Using TTL analog sensor can be slow as the micro-controller needs to perform DAC (digital-to-analog converter).

Overall, the analog sensor will be replaced by a new sensor in next prototype because it is the most important hardware for anti-sway algorithm.

Summarily, by using a relatively inexpensive and available hardware, the first generation anti-sway prototype has been built and proven to be effective in cancelling crane's sway.

8. SECOND GENERATION PROTOTYPE WITH DSPIC33F

8.1. Introduction

The second generation design of the device is created based on testing results of the first generation anti-sway prototype. The second generation prototype will be very similar to final production product. The design improvements will include:

- dsPIC33F Microcontroller Family from Microchip Technology is selected as new MCU for the board.
- ADIS16209 from Analog Devices, Inc is selected as our new inclination sensor superseding previous noisy analog sensor.

The purposes of these improvements include:

- Giving developers more control over the board.
- Boosting performance and precision.
- Protecting signals against noise.
- Adding new functionality to the board in addition to original anti-sway feature.

8.2. dsPIC33F Microcontroller Family

dsPIC33F MCUs from Microchip Technology belong to high-performance 16-bit digital signal controller family. The dsPIC33F MCU is equipped with Digital Signal Processing (DSP) capacity. As a result, the dsPIC33F MCU can provide very high computation and throughput capacities.

“A Digital Signal Controller (DSC) is a single-chip, embedded controller that seamlessly integrates the control attributes of a Microcontroller (MCU) with the computation and throughput capabilities of a Digital Signal Processor (DSP) in a single core.”(Microchip Technology, dsPIC® Digital Signal Controllers The Best of Both Worlds, 2005).

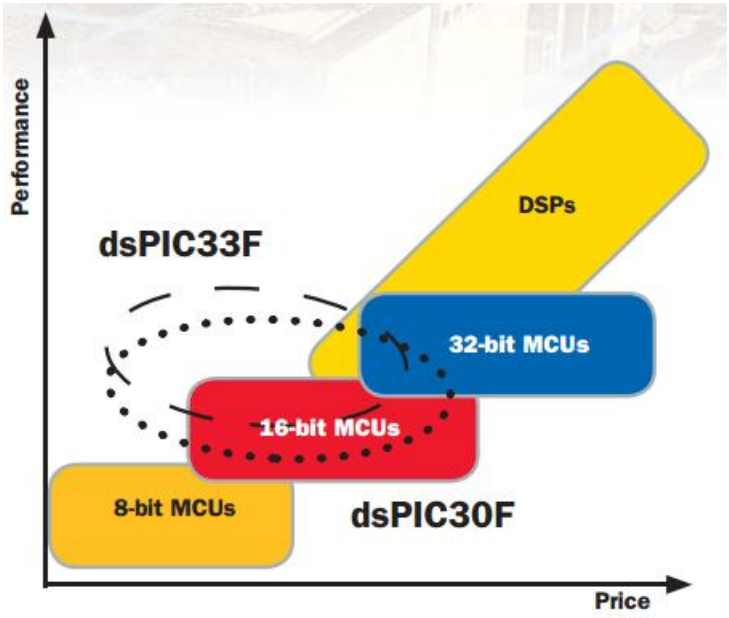

Figure 67. dsPIC33F Performance vs. Price chart (Microchip Technology, 2005. *dsPIC® Digital Signal Controllers the Best of Both Worlds*).

dsPIC33F distinguished features:

- Maximum CPU Speed: 40 million instructions per second (MIPS).
- Operating temperature: (-40° to 85° C).
- 8 channel DMA.
- Up to 85 programmable digital I/O pins. Programmable pins make the hardware design much simpler. Every programmable pin can be assigned different functionality (UART, analog IO, digital IO, SPI, etc…). In another words, pin functionality is defined by software.
- Built-in Internal RC Oscillator.
- Dedicated I²C module.
- Multiple protocol supports: UART, SPI, I2C, CAN, PMP (Parallel Master Port) Parallel Port.

(Microchip Technology, 2006. *dsPIC33F Family Data Sheet*).

Following dsPIC33F MCUs have been tested during the project:

- dspic33FJ128MC802 which is 28-pin version of dsPIC33F family.
- dsPIC33FJ64MC804 which is 44-pin version of dsPIC33F family.

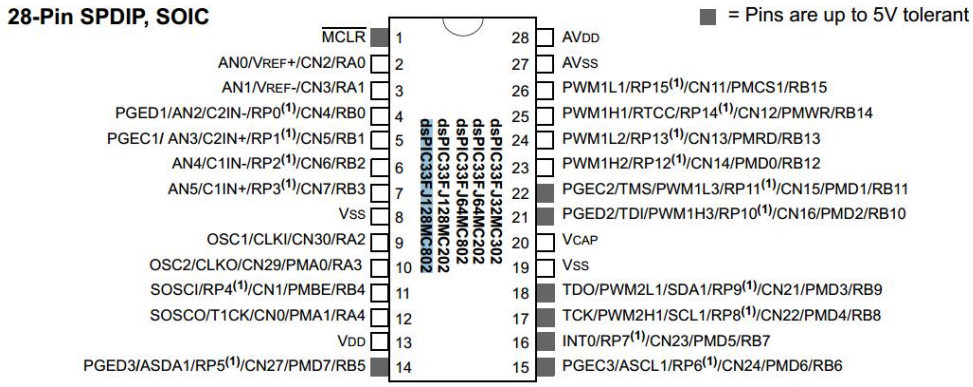

Figure 68. dsPIC33FJ128MC802 (Microchip Technology.*dsPIC33FJ32MC302/304, dsPIC33FJ64MCX02/X04 and dsPIC33FJ128MCX02/X04*).

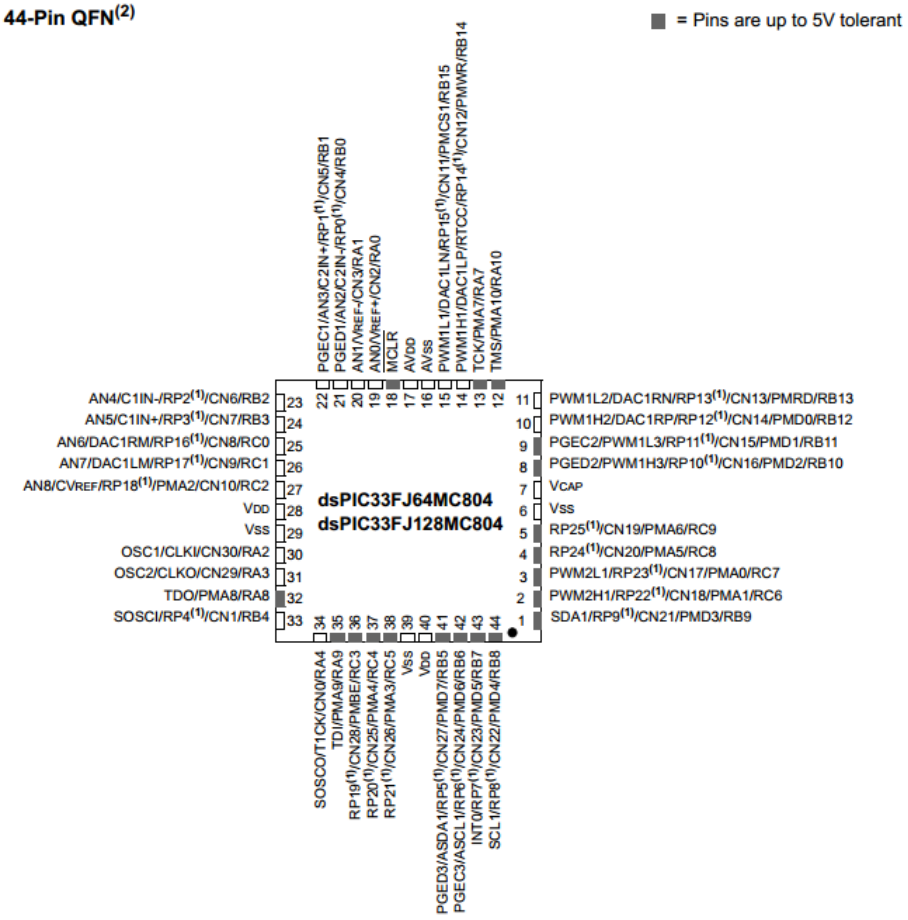

Figure 69. dsPIC33FJ64MC804 (Microchip Technology. *dsPIC33FJ32MC302/304, dsPIC33FJ64MCX02/X04 and dsPIC33FJ128MCX02/X04*).

Both tested MCUs have shown great flexibilities and computational capacities. Especially, by using programmable pin feature, the same software can run in both mentioned MCU without any changes.

8.3. ADIS16209 digital multi-purpose sensor

ADIS16209 from Analog Devices is high accuracy, dual-axis digital inclinometer and accelerometer. The sensor operates on 3.3 V and communicates with MCU via SPI (Serial Peripheral Interface Bus).

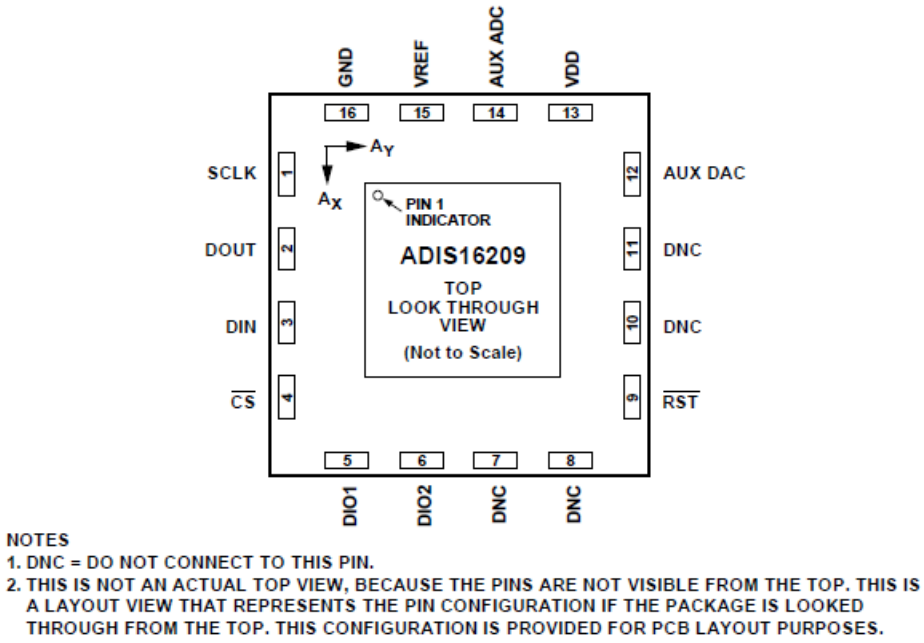

Figure 70. ADIS16209 pin configuration (Analog Devices, ADIS16209 data sheet).

In addition to measuring inclinations, ADIS16209 is capable of measuring dual-axis accelerations and temperature. These additional capabilities of the sensor make anti-sway board even more versatile.

Most notable features of ADIS16209:

- High accuracy, 0.1°.
- Digital inclination data, 0.025° resolution.
- Digital acceleration data, 0.244 mg resolution.
- ±1.7 g accelerometer measurement range.
- Digitally controlled bias calibration.
- Digitally controlled sample rate.
- Digitally controlled frequency response.

The sensor is working based on request/response mechanism. The MCU sends read/write requests to the sensor via SPI protocol and sensor will perform actions based on original requests. For full list of possible request registers, please refer to table User Register Map in “Analog Devices, ADIS16209 Data Sheet”.

In comparison to previous analog ASM PTAM27, ADIS16209 holds several advantages:

- ADIS16209 has built-in ADC (analog-to-digital converter).
- The SPI communication protocol of ADIS16209 is more robust than analog channel.
- ADIS16209 has mechanism to correct known sources of errors that would otherwise reduce accuracy level.
- ADIS16209 is more versatile with its acceleration and temperature measuring capabilities.

8.4. Remote pendant integration

For normal remote pendant configuration in ABB ACS800 is as follow:

Table 9. Remote pendant configuration parameters for ACS800.

Parameter	Value	Description
Parameter 10.01 EXT1 STRT/STP/DIR	DI1 F, DI2 R	Digital Input 1 for forward direction, Digital Input 2 for reverse direction.
12.01 STEP REF SEL	DI3,4,5	Digital Input 3, 4 and 5 are used to change to different speed.
12.02 STEP REF 1 [rpm]	For example: 500.	This speed is enabled if DI3, DI4 and DI5 are low.
12.03 STEP REF 2 [rpm]	For example: 1000.	This speed is enabled if DI3 is high.

12.04 STEP REF 3 [rpm]	For example: 1500.	This speed is enabled if DI3 and DI4 are high.
12.05 STEP REF 3 [rpm]	For example: 2000.	This speed is enabled if DI3, DI4 and DI5 are high.

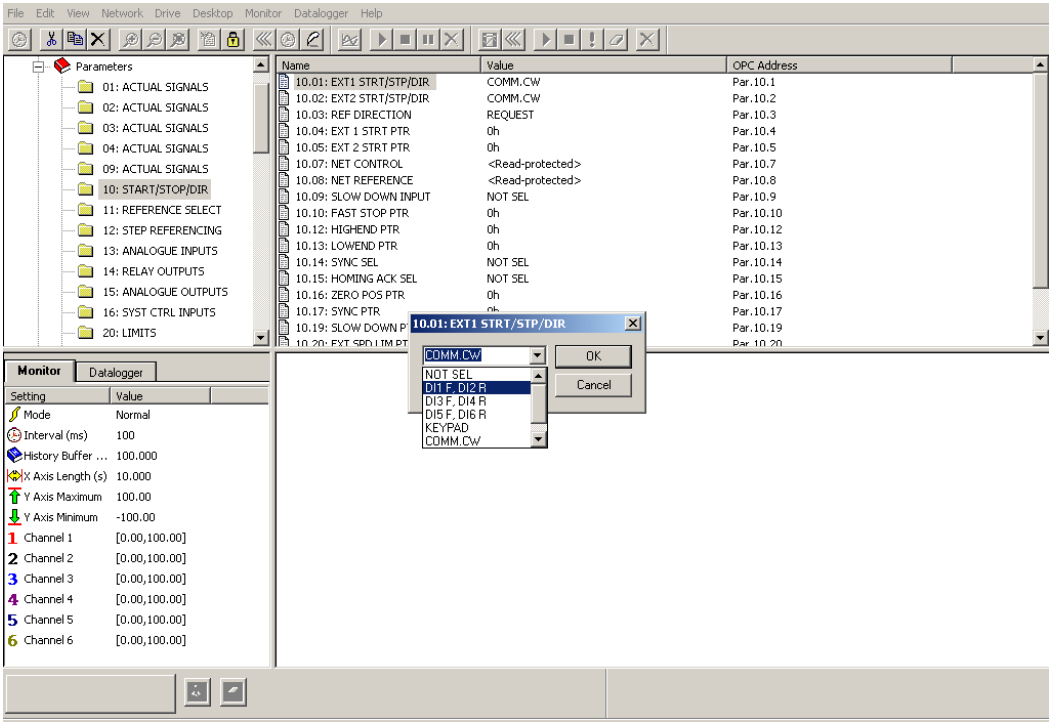

Figure 71. Remote pendant direction configuration.

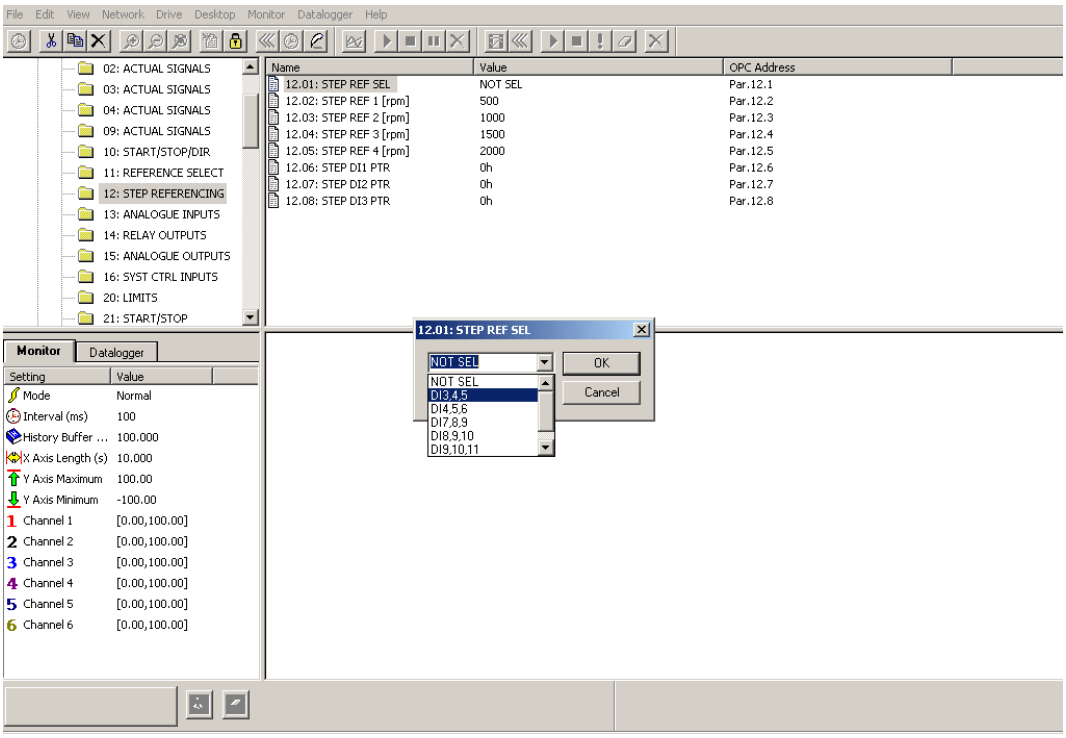

Figure 72. Remote pendant speed configuration.

For first generation board, the crane is started and stopped using buttons on the board directly. However, for production usage, the remote pendant must be the device to start and stop crane. Therefore, the remote pendant integration module must be implemented.

In second generation prototype, the remote pendant integration module is implemented by reading parameters from the motor drive. Firstly, the ABB ACS800 is configured to enable Modbus control and disable remote pendant control as in "5.3. Modbus configuration for ACS800". Then during start-up, the board will read and store parameter 12.02, 12.03, 12.04 and 12.05 values in memory. The anti-sway constantly listens for changes in value of digital inputs by reading parameter 1.17 DIL DI6–1 STATUS and comparing with "Table 1. Remote pendant configuration parameters." By detecting changes of 1.17 parameter, the board is able to decide pendant actions such as start or stop signal. Moreover, the target speed is also detected by reading DI3, DI4 and DI5. As the result, the anti-sway board is able to act accordingly with user's actions on the pendant.

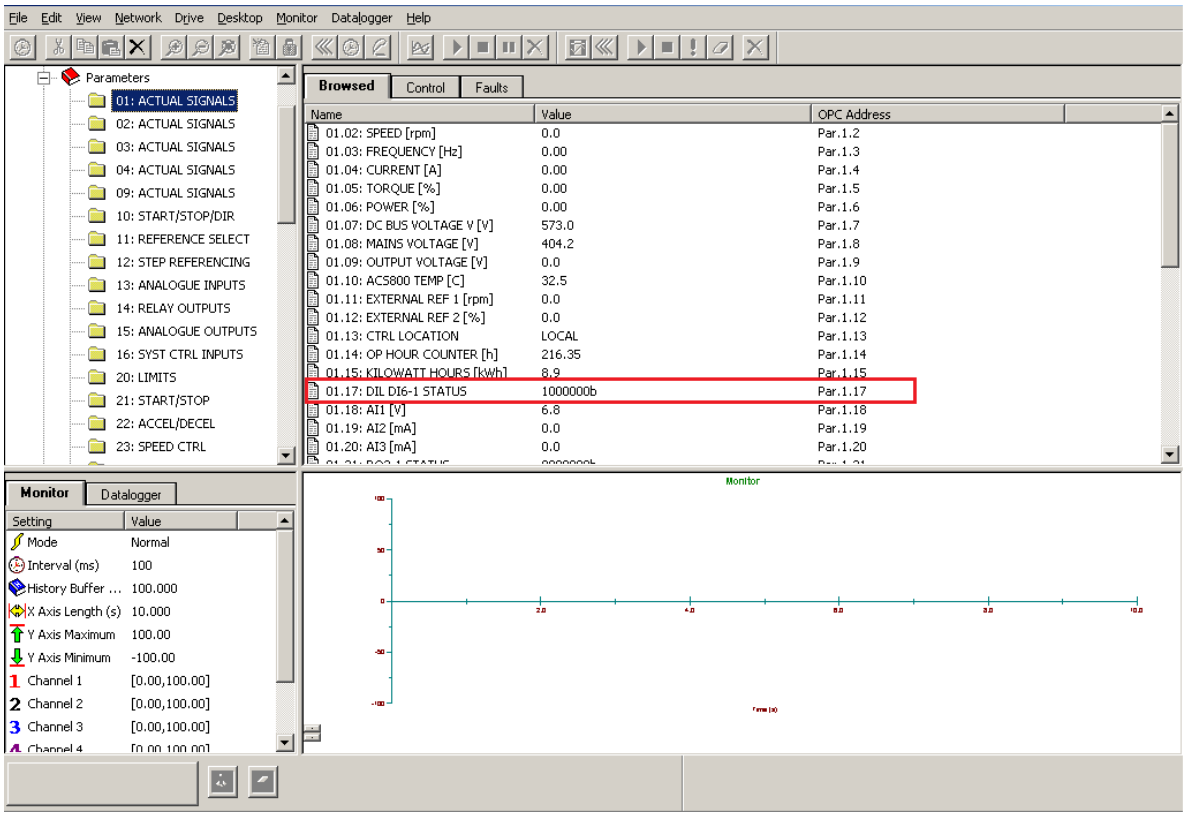

Figure 73. Parameter 01.17 DIL DI6-1 STATUS.

8.5. Second generation prototype board

The board is built on breadboard to validate original design.

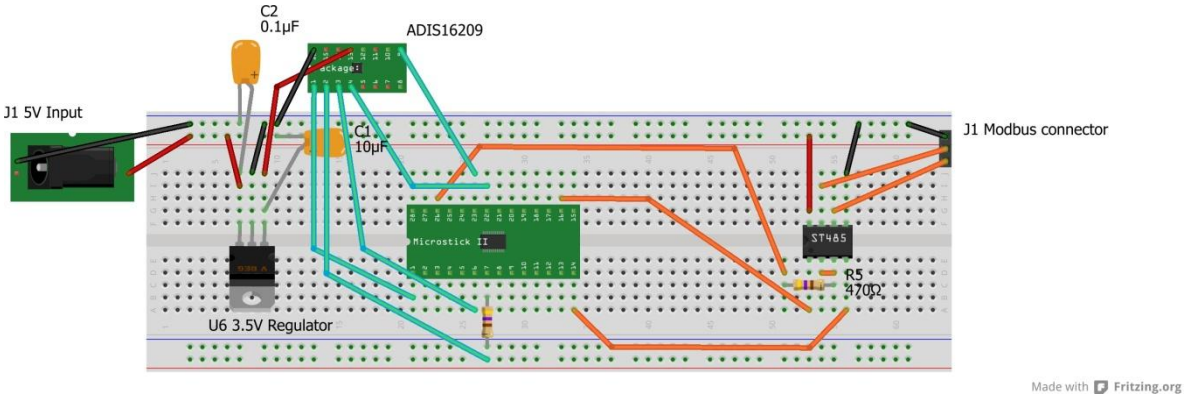

Figure 74. Second generation anti-sway prototype design.

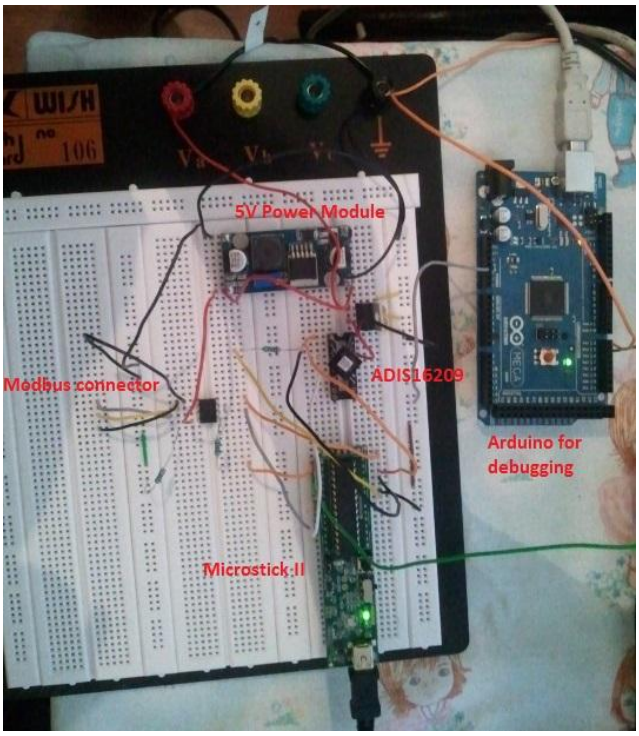

Figure 75. Second generation anti-sway protoboard.

The board was successfully validated against the ACS800 test rack. In this prototype board, Microstick II which is integrated development hardware platform for Microchip's 16-bit and 32-bit microcontrollers was used to develop software on the MCU. Modbus, remote pendant integration and SPI drivers are successfully implemented on dsPIC33F platform. All anti-sway requirements are strongly fulfilled by the design.

8.6. Production board

A short introduction of final production board will be given in this section of this thesis. The final production board is highly similar in design with second generation prototype. Improved features of production boards include:

- EEPROM (Electrically Erasable Programmable Read-Only Memory) is needed to store sensor's calibration parameters, logging data and different motor step speeds.

- ADM2582E from Analog Devices, Inc is selected as our new RS-485 Transceiver. The signal and power of RS-485 signal is isolated. Therefore, better transmission of Modbus is guaranteed.
- Ethernet support. Ethernet communication will be supported for future features. Microchip TCP/IP stack (Microchip Technology Inc, The Microchip TCP/IP Stack) has been successfully customized and flashed to production board. The board can act as standard HTTP server, FTP server or TCP/IP client, etc.
- Better power module to provide protection against power outage.
- Instead of using imprecise internal oscillator of dsPIC33F, crystal oscillator is used as clock source for better accuracy.
- The sensor is attached directly to the board. As the result, whole board will be attached to the static part of the crane's rope.

Figure 76. Final anti-sway production board (with Ethernet and 2 Modbus ports).

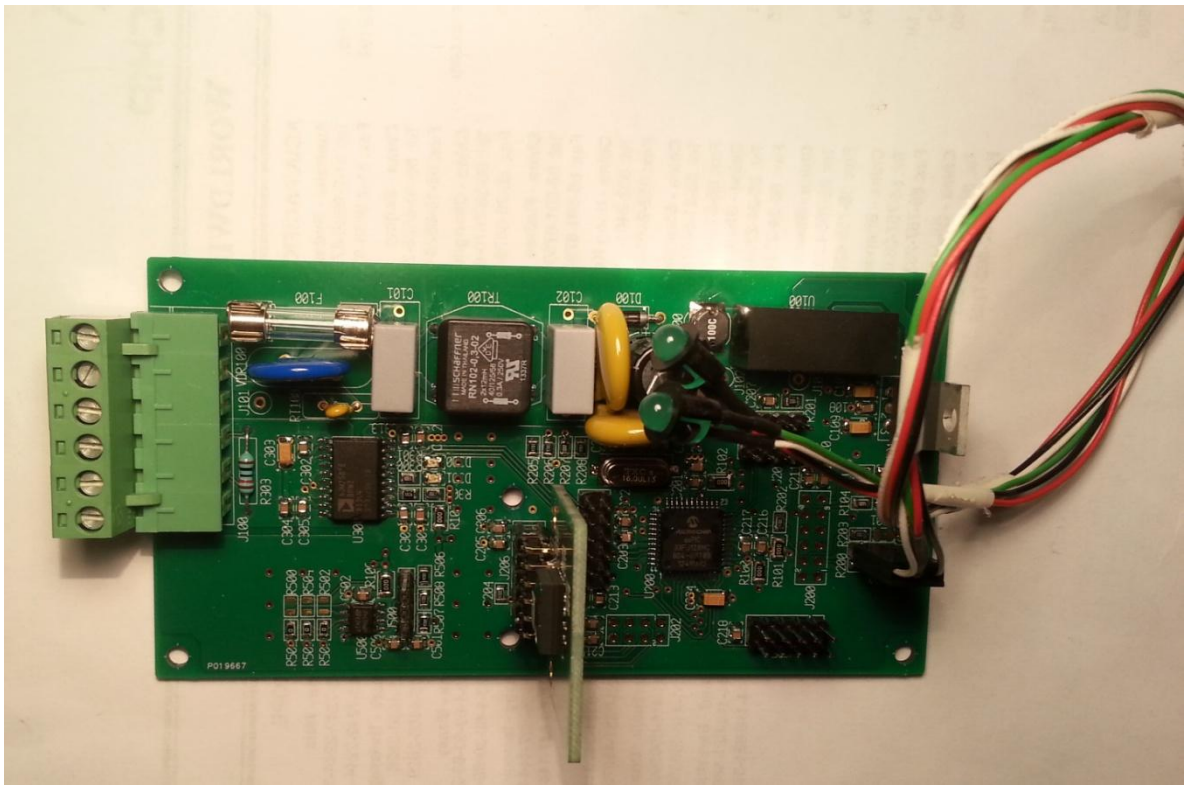

Figure 77. Final anti-sway production board (without Ethernet and only one Modbus port).

8.7. Conclusion and testing results

In this chapter, the second generation and production anti-sway devices were designed using dsPIC33F from Microchip Technology as MCU. The dsPIC33F family is more computationally powerful and gives developers greater control over functionalities of the MCU. The inclination sensor, the most important component of anti-sway board, is also switched to digital ADIS16209 inclination sensor which provides much more functionalities and robustness. Moreover, software module for integrating with crane's remote pendant is implemented. In addition to second generation board design, the final production board functionalities and improvements were briefly introduced.

The effectiveness of anti-sway solution is demonstrated by following videos which were recorded during test session.

- Crane movement without anti-sway support:

  http://youtu.be/ymtF1NXh8fE

- Crane movement in single direction(with anti-sway support):

  http://youtu.be/krzeWyu0JJM

  http://youtu.be/a-Qt9K2yXhM

- Crane movement in both directions(with anti-sway support):

  http://youtu.be/B6X-sblZ1NI

  http://youtu.be/Q5tB2DLaEXs

- Initial sway at the beginning of crane's movement(with anti-sway support):

  http://youtu.be/fdQmEl9V8w8

Following graphs were captured when operating crane with and without anti-sway device:

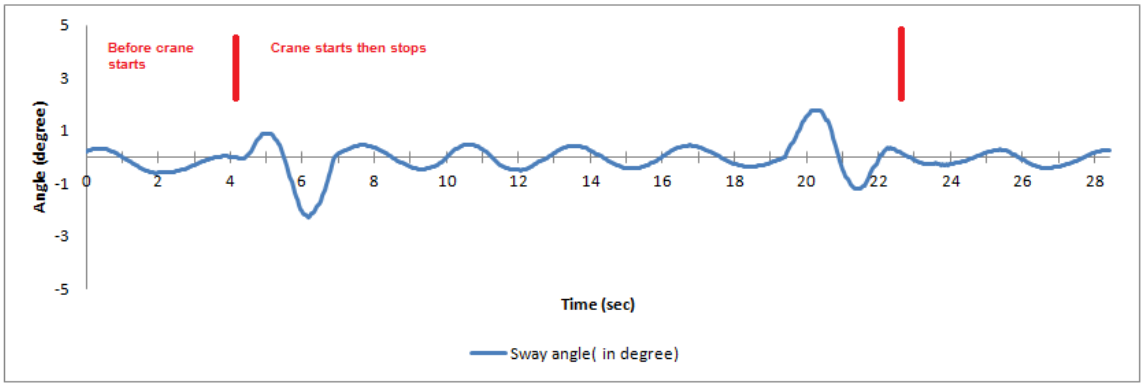

Figure 78. Sway angle when using anti-sway device.

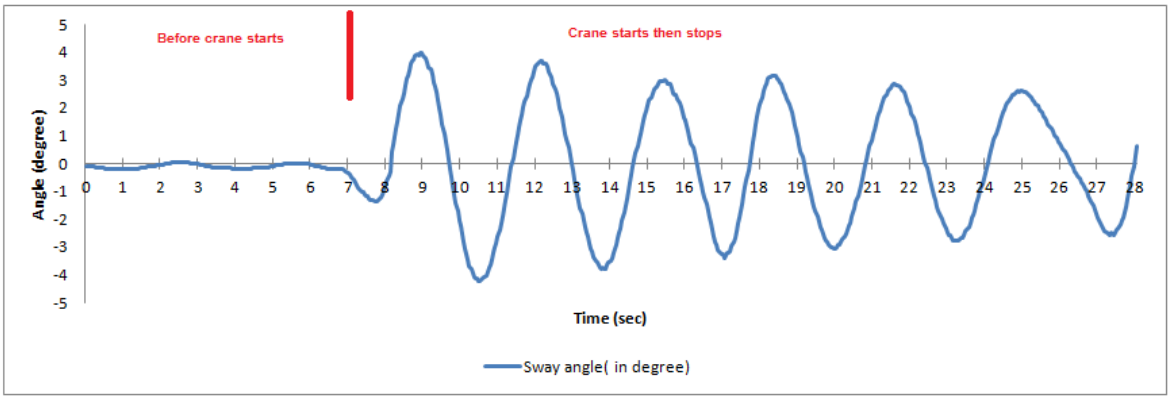

Figure 79. Sway angle without anti-sway device.

As in Figure 77, after ramping up (acceleration) and ramping down (deceleration) period, the crane moves very stable (with almost no oscillation). In contrast, in Figure 78, the crane remains swinging heavily during and after crane's movement. Moreover, with anti-sway device, the sway is killed off very fast in comparison with previous works mentioned in *1.3. Overview of related works*.

9. CONCLUSION AND FUTURE WORK

In this thesis, the swinging nature of overhead cranes has been discussed in depth in order to come up with an effective anti-sway solution. Physics model of overhead crane has been built in order to simulate swinging behavior in physics engine. Box2D framework was selected as physics engine to study swinging phenomenon during crane's movement. Based on the research and simulation of crane model, a novel crane anti-sway solution was proposed. The solution combines both hardware and software to solve swinging problem. Apart from being able to effectively reduce sway, the proposed solution also satisfies following additional requirements:

- Independence of load weight.
- Independence of crane rope length.
- Fast convergence, sway is reduced very rapidly.
- Easy to deploy and maintain.
- Easy to extend to perform additional functionalities.

The anti-sway solution has been successfully built and tested in simulated environment as well as real industrial environment. Two prototype designs have been built and tested during the project before producing production board.

The final anti-sway board can be considered as multi-purposed hardware. It can be extended easily to perform additional tasks such as:

- Monitoring device over Internet: monitor different values (environment temperature, crane acceleration and crane parameters, etc) and send them over TCP/IP to server.
- Device control over Internet such as: start/stop crane, changing speed, etc.

Moreover, thanks to the multi-purpose sensor, anti-sway device can perform many advanced features:

- Collision detection: by using inclination and acceleration readings from sensors to monitor if there is collision happens with the load.
- Straight lift or drop of load: by using inclination readings, the crane is able adjust/move to correct angle of the rope while lifting the load.
- Move the crane by using forced controlled pushing: operator can move the crane by apply a small amount of pushing force to the load to create an angle, then crane will slowly move accordingly to the direction of the pushing force.

In short, the limit of the board is up to our imagination. With TCP/IP and multi-purpose sensor support, the anti-sway device is able to perform many operations that can greatly enhance the safety and effectiveness of crane operations.

Currently, the board only supports anti-sway functionality for indoor cranes and cranes that suffers from constant wind. For future work, we will continue to perform research with outdoor cranes.

REFERENCE

David Morin (2008). *Introduction to Classical Mechanics.* Cambridge University Press. ISBN: 9780521876223.

Randall D. Knight (2012). *Physics for Scientists and Engineers: A Strategic Approach with Modern Physics, 3/E*. Pearson Education, Inc. ISBN-10: 0321844351.

M.A. Ahmad (2009). *Sway Reduction on Gantry Crane System using Delayed Feedback Signal and PD-type Fuzzy Logic Controller: A Comparative Assessment.* Proceedings of World Academy of Science, Engineering And Technology Volume 38 February 2009. ISSN: 2070-3740.

Y. S. Kim, K. S. Hong and S. K. Sul (2004). *Anti-Sway Control of Container Cranes: Inclinometer,Observer, and State Feedback*. International Journal of Control, Automation, and Systems, Vol.2.

G. Bartonlini, A. Pisano and E. Usai (2002). *Second-order sliding-mode control of container cranes.* Automatica, Vol. 38.

Y. Fang, W. E. Dixon and D. M. Dawson, E. Zergeroglu (2003). *Nonlinear coupling control laws for an underactuated overhead crane system.* IEEE/ASME Trans. Mechatron, Vol.8.

W. Wang, J. Yi, D. Zhao and D. Liu (2004). *Design of a stable sliding-mode controller for a class of second-order underactuated systems*. IEE Proceedings - Control Theory and Applications.

K. S. Hong, B. J. Park, and M. H. Lee (2000). *Two stage control for container cranes.* JSME International Journal, Series C, vol. 43.

Kim, Y.S., Yoshihara, H., Fujioka, N., Kasahara, H., Shim, H. and Sul, S.K (2003). *A new vision-sensorless anti-sway control system for container cranes*. Industry Applications Conference, Vol. 1.

Neil Singer, William Singhose and Eric Kriikku(1997) . *An Input Shaping Controller Enabling Cranes to Move without Sway.* American Nuclear Society 7th Topical Meeting on Robotics and Remote Systems.

Ki-Ru Park and Dong-Soo Kwon (2010). *Swing-Free Control of Mobile Harbor Crane with Accelerometer Feedback.* International Conference on Control, Automation and Systems 2010.

Rajeeb Dey, Nishant Sinha, Priyanka Chaubey, S. Ghosh and G. Ray (2010). *Active Sway Control of a Single Pendulum Gantry Crane System using Output-Delayed Feedback Control Technique*. 2010 11th Int. Conf. Control, Automation, Robotics and Vision.

Kitichoke Prommaneewat, Prapas Roengruen and Viriya Kongratana (2007). *Anti-sway Control for Overhead Crane*. International Conference on Control, Automation and Systems.

Hideki Kawai, Young Bok Kim and Yong Woon Choi (2009). *Anti-sway system with image sensor for container cranes*. Journal of Mechanical Science and Technology 23.

Shu-jiang Li, zhi-yuan Xu, Hai Wu, Shao-hua Hu and Jin-xue Xu(2005). *Intelligent anti-swing control for horizontal moving process of bridge crane*. International Conference on Control and Automation.

Dong Kyu Kim, Young Bok Kim, Ji Seong Jang and Guisheng Zhai (2005). *Gain-Scheduling Approach to Mass Damper Type Anti-Sway System Design*. Proceedings of the 16th IFAC World Congress, 2005.

GB. Kang, Y.B. Kim, S.B.An, G.H. Chae and J.H. Yang (2003). *A New Approach to Anti-Sway System Design for a Container Crane*. SICE Annual Conference.

Dah-Jing Jwo (2007). *Remarks on the Kalman filtering simulation and verification*. Applied Mathematics and Computation 186 (2007).

Baoding Weyou Technology Company. *EOT Crane* [online]. Accessed 18 August 2013, <http://www.weyou.co/info2/info25.html>.

U.S. Department of Energy (2007). *DOE Standard Hoisting and Rigging.*

Greg Welch and Gary Bishop (2006). *An Introduction to the Kalman Filter.*

Ramsey Faragher (2012). *Understanding the Basis of the Kalman Filter Via a Simple and Intuitive Derivation.* IEEE Signal Processing Magazine.

The Modbus Organization(2002). *MODBUS over Serial Line Specification & Implementation guide V1.0.*

ABB Group. *ABB industrial drives ACS800, single drives, 0.75 to 6000 hp.*

ABB Group (2009). *ACS800 Firmware Manual ACS800 Standard Control Program 7.x.*

ABB Group (2002). *Modbus Adapter Module RMBA-01 User's Manual.*

ASM GmbH. *Sensors and Encoders for Angle and Inclination.*

ASM GmbH. *PTAM27 Universal MEMS Inclination Sensor with Analog Output.*

STMicroelectronics (2000). *Low Power Rs-485/Rs-422 Transceiver.*

Analog Devices, Inc . *High Accuracy, Dual-Axis Digital Inclinometer and Accelerometer ADIS16209 Rev.C.*

ABB Group (2005). *Adaptive Program Application Guide.*

Microchip Technology Inc (2011). *Microstick II Information Sheet.*

Microchip Technology Inc (2004). *dsPIC® Language Tools Libraries.*

Microchip Technology Inc (2012). *dsPIC33FJ32MC302/304, dsPIC33FJ64MCX02/X04 and dsPIC33FJ128MCX02/X04 16-bit Digital Signal Controllers (up to 128 KB Flash and 16K SRAM) with Motor Control PWM and Advanced Analog.*

Nilesh Rajbharti, Microchip Technology Inc (2008). *The Microchip TCP/IP Stack.*

Martin Bowman Microchip Technology Inc (2007). *Using the C30 Compiler and the I2C™ Peripheral to Interface Serial EEPROMs with dsPIC33F.*

Erin Catto (2011). *Box2D v2.2.0 User Manual.*

Arduino project. *Arduino Language Reference* [online]. Accessed 18 August 2013, < http://arduino.cc/en/Reference/HomePage>.

Microchip Technology Inc (2009). *Section 23. Serial Peripheral Interface (SPI).*

Microchip Technology Inc (2006). *Section 24. Inter-Integrated Circuit™ (I2C™)*

Loughborough Sound Images (1997). *Evaluation of the performance of the c6201 processor &compiler.*

Hyeokho Choi(2003). *Fixed Point Arithmetic.*